

# bradscholars

## ARID3B: A novel regulator of the Kaposi's sarcoma-associated herpesvirus lytic cycle

Item Type	Article
Authors	Wood, J.J.;Boyne, James R.;Paulus, C.;Jackson, B.R.;Nevels, M.M.;Whitehouse, A.;Hughes, D.J.
Citation	Wood JJ, Boyne JR, Paulus C, Jackson BR et al (2016) ARID3B: A novel regulator of the Kaposi's sarcoma-associated herpesvirus lytic cycle. Journal of Virology. 90(20): 9543–9555.
DOI	<a href="https://doi.org/10.1128/JVI.03262-15">https://doi.org/10.1128/JVI.03262-15</a>
Rights	2016 Wood et al. This is an open-access article distributed under the terms of the Creative Commons Attribution 4.0 International license ( <a href="http://creativecommons.org/licenses/by/4.0/">http://creativecommons.org/licenses/by/4.0/</a> ).
Download date	2026-06-13 00:49:21
Link to Item	<a href="http://hdl.handle.net/10454/8805">http://hdl.handle.net/10454/8805</a>



# The University of Bradford Institutional Repository

<http://bradscholars.brad.ac.uk>

This work is made available online in accordance with publisher policies. Please refer to the repository record for this item and our Policy Document available from the repository home page for further information.

To see the final version of this work please visit the publisher's website. Access to the published online version may require a subscription.

**Link to publisher's version:** <http://dx.doi.org/10.1128/JVI.03262-15>

**Citation:** Wood JJ, Boyne JR, Paulus C, Jackson BR et al (2016) ARID3B: A novel regulator of the Kaposi's sarcoma-associated herpesvirus lytic cycle. *Journal of Virology*. 90(20): 9543-9555.

**Copyright statement:** © 2016 Wood et al. This is an open-access article distributed under the terms of the [Creative Commons Attribution 4.0 International license](https://creativecommons.org/licenses/by/4.0/).

1 **ARID3B: A novel regulator of the Kaposi's sarcoma-associated herpesvirus lytic cycle**

2 Jennifer J Wood,<sup>a</sup> James R Boyne,<sup>c</sup> Christina Paulus,<sup>d</sup> Brian R Jackson,<sup>a,b</sup> Michael M Nevels,<sup>d</sup>  
3 Adrian Whitehouse,<sup>a,b,#</sup> David J Hughes,<sup>d,#</sup>

4

5 School of Molecular and Cellular Biology<sup>a</sup> and the Astbury Centre for Structural Molecular  
6 Biology<sup>b</sup>, Faculty of Biological Sciences, University of Leeds, Leeds, UK; Centre for Skin Sciences,  
7 University of Bradford, Bradford, UK<sup>c</sup>; Biomedical Sciences Research Complex, University of St.  
8 Andrews, St. Andrews, UK<sup>d</sup>

9

10 Running title: ARID3B inhibits the KSHV lytic cycle

11 #Address correspondence to:

12 David J Hughes [djh25@st-andrews.ac.uk](mailto:djh25@st-andrews.ac.uk), Adrian Whitehouse [a.whitehouse@leeds.ac.uk](mailto:a.whitehouse@leeds.ac.uk)

13 J.J.W. and J.R.B. contributed equally to this work.

14

15

16 Abstract word count: 248

17 Main text word count: 7666

18 **Abstract**

19 KSHV is the causative agent of commonly fatal malignancies of immuno-compromised individuals,  
20 including primary effusion lymphoma (PEL) and Kaposi's sarcoma (KS). A hallmark of all  
21 herpesviruses is their biphasic lifecycle – viral latency and the productive lytic cycle, and it is well  
22 established that reactivation of the KSHV lytic cycle is associated with KS pathogenesis. Therefore,  
23 a thorough appreciation of the mechanisms that govern reactivation is required to better  
24 understand disease progression. The viral protein, replication and transcription activator (RTA),  
25 is the KSHV lytic switch protein due to its ability to drive the expression of various lytic genes,  
26 leading to reactivation of the entire lytic cycle. While the mechanisms for activating lytic gene  
27 expression have received much attention, how RTA impacts on cellular function is less well  
28 understood. To address this, we developed a cell line with doxycycline-inducible RTA expression  
29 and applied SILAC-based quantitative proteomics. Using this methodology, we have identified a  
30 novel cellular protein (AT-rich interacting domain containing 3B, ARID3B) whose expression was  
31 enhanced by RTA and that relocalised to replication compartments upon lytic reactivation. We  
32 also show that siRNA knockdown or overexpression of ARID3B led to an enhancement or  
33 inhibition of lytic reactivation, respectively. Furthermore, DNA affinity and chromatin  
34 immunoprecipitation assays demonstrated that ARID3B specifically interacts with A/T-rich  
35 elements in the KSHV origin of lytic replication (oriLyt), and this was dependent on lytic cycle  
36 reactivation. Therefore, we have identified a novel cellular protein whose expression is enhanced  
37 by KSHV RTA with the ability to inhibit KSHV reactivation.

38 **Importance**

39 Kaposi's sarcoma-associated herpesvirus (KSHV) is the causative agent of fatal malignancies of  
40 immunocompromised individuals, including Kaposi's sarcoma (KS). Herpesviruses are able to  
41 establish a latent infection, where they escape immune detection by restricting viral gene  
42 expression. Importantly however, reactivation of productive viral replication (the lytic cycle) is  
43 necessary for the pathogenesis of KS. Therefore, it is important that we comprehensively  
44 understand the mechanisms that govern lytic reactivation, to better understand disease  
45 progression. In this study, we have identified a novel cellular protein (AT-rich interacting domain  
46 protein 3B, ARID3B) that we show is able to temper lytic reactivation. We showed that the  
47 master lytic switch protein, RTA, enhanced ARID3B levels, which then interacted with viral DNA  
48 in a lytic cycle dependent manner. Therefore, we have added a new factor to the list of cellular  
49 proteins that regulate the KSHV lytic cycle, which has implications for our understanding of KSHV  
50 biology.

51

## 52 **Introduction**

53 Infection of immune-compromised people with Kaposi's sarcoma-associated herpesvirus (KSHV)  
54 is frequently linked with fatal malignancies. It is well established as the causative agent of primary  
55 effusion lymphoma (PEL) and Kaposi's sarcoma (KS) and is often associated with multicentric  
56 Castleman's disease (MCD) (1, 2). Like all herpesviruses, KSHV infection is lifelong and has two  
57 distinct phases to its life cycle; latency and the lytic cycle. Latency is associated with a highly  
58 restrictive viral gene expression program involving the latency-associated nuclear antigen (LANA),  
59 viral FLICE inhibitory protein (vFLIP), viral cyclin, kaposin and various virally-encoded miRNAs and  
60 together, these are required for maintenance of the KSHV genome *in vitro* (3) and tumorigenesis  
61 *in vivo* (2). However, reactivation from latency to the lytic cycle is indispensable for the  
62 pathogenesis of KS; indeed active virus replication and increased viral loads are associated with  
63 poorer clinical outcomes (4-6) and, there is clinical evidence that treatment of patients with  
64 ganciclovir (inhibitor of herpesvirus replication) significantly reduces the incidence of KS (7).  
65 Therefore, a comprehensive understanding of molecular mechanisms that govern KSHV  
66 reactivation is critical to our understanding of disease progression.

67 Expression of a single viral protein, replication and transcriptional activator (RTA), is both  
68 necessary and sufficient for reactivation of the KSHV lytic cycle (reviewed in (8)). *In vitro*, RTA  
69 expression is stimulated by certain cellular cues such as plasma cell differentiation (9, 10) and  
70 hypoxia (11), and because RTA autoactivates its own promoter and drives the full lytic cycle, it is  
71 well established as the true KSHV lytic-switch protein (8). RTA activates transcription of lytic  
72 genes by directly interacting with RTA-responsive elements (RREs) found in some lytic gene

73 promoters, or indirectly via interactions with cellular transcription factors, particularly RBP-Jκ,  
74 AP-1 and Oct-1 (8). The RTA protein comprises all the elements that one would expect for a  
75 transcriptional activator, such as nuclear localization signals (NLS), a DNA binding domain (DBD)  
76 and a transcriptional activation (TA) domain. Further functional domains have also been  
77 identified, such as a leucine zipper domain that is important for homo-tetramer formation (12),  
78 a serine/threonine-rich region that is subject to phosphorylation (13) and a multitude of binding  
79 sites for various protein-protein interactions (PPIs) (8).

80 The best characterized lytic promoters that are dependent on the direct DNA binding mechanism  
81 are the PAN and K12 promoters (14, 15). Both genes are highly expressed during lytic reactivation,  
82 but their expression is prevented when DNA binding mutants of RTA are expressed (15).  
83 Furthermore, transfection experiments with plasmids containing the PAN promoter showed that  
84 RTA was essential for activating transcription, as mRNA was undetectable in its absence (16). The  
85 sequence elements that were found to be RTA-responsive demonstrated significant homology  
86 between the PAN and K12 promoters, and centered on an A/T-rich trinucleotides (17)  
87 reminiscent of interferon-stimulated response elements found in the promoters of interferon-  
88 dependent genes (18).

89 There are several lytic genes that are activated via the indirect mechanism, including the RTA  
90 gene itself (*ORF50*), *ORF57 (Mta)*, *ORF6*, *ORF74 (vGCPR)*, *K6 (vMIP-1)*, and *ORF73 (LANA)* (15, 19,  
91 20). However, whether RTA's intrinsic DNA binding property is important for the activation of  
92 promoters via the indirect mechanism is a contentious issue. While some view that RTA's ability  
93 to transactivate the *ORF57* promoter is completely dependent on PPIs (15), others suggest that

94 cooperation between RTA-DNA interactions and PPIs enhances the activation of transcription.  
95 For example, in addition to the essential RBP-J $\kappa$  binding site found in the ORF57 promoter, RTA  
96 binding sites have been identified that surround this region that have been characterized as  
97 partial palindromes of A/T-rich elements with a 5'-CANT-3' (N = any nucleotide) repeat core  
98 element (21). Extensive analysis of this promoter element suggested a model whereby RTA  
99 recruits RBP-J $\kappa$  to its consensus binding sequence, and through tetramer formation, RTA makes  
100 contacts with its cognate CANT-repeats (21). Furthermore, stabilization of this complex may  
101 occur via further upstream CANT-repeat interactions involving additional cellular transcription  
102 factors, such as AP-1 (8).

103 RTA is also required to coordinate lytic replication of the KSHV genome at the *cis*-acting origins  
104 of lytic replication (oriLyt). For example, it is responsible for docking the viral pre-replication  
105 complex at the oriLyt (22), and this process, for unknown reasons, requires RTA-mediated  
106 transcription of an oriLyt-associated transcript (23, 24). Two distinct oriLyt sequences have been  
107 identified in the KSHV genome (oriLyt left and right); interestingly, RREs in oriLyt left share  
108 significant homology to those found in the PAN and K12 promoters (23). Furthermore, oriLyt  
109 contains an A/T-rich region consisting of various palindromic sequences in addition to a highly  
110 G/C-rich repeat element. Interestingly, DNA affinity studies have demonstrated that several  
111 cellular proteins preferentially interact with oriLyt via its A/T-rich regions (25).

112 Unlike most other herpesviruses, *de novo* infection of cells lines with KSHV leads to latency where  
113 the viral genome is rapidly chromatinized and lytic genes are associated with repressive histone  
114 modifications (26-28), making KSHV an amenable model for studying the establishment of

115 herpesvirus latency. Furthermore, reactivation of the lytic cycle promotes various negative  
116 feedback mechanisms that serve to temper lytic gene expression during reactivation and, *in vivo*,  
117 these presumably function to promote the establishment or maintenance of latency. These  
118 include viral factors (e.g. LANA (29, 30) and viral miRNAs (31)) and cellular proteins (e.g. NF- $\kappa$ B  
119 (32), TLE2 (33), PARP-1 (34) and HDAC1 (35)) which have been found to temper RTA  
120 transactivation of its target promoters and thus reactivation of the lytic cycle. Clearly, silencing  
121 of KSHV lytic gene expression, or inhibition of lytic DNA replication, is an important step in the  
122 life cycle of KSHV. Nevertheless, the mechanisms that are involved are poorly understood.

123 To begin to gain an understanding of how RTA expression impacts on the cellular proteome, we  
124 employed a global quantitative proteomics approach using stable isotope labeling of amino acids  
125 in cell culture coupled to tandem mass spectrometry (SILAC-MS/MS). Quantitative proteomics,  
126 using various platforms, is a powerful method that has been employed by various laboratories,  
127 including our own (36-38), to investigate virus-host interactions (recently reviewed in (39) and  
128 (40)). Using this approach we identified a novel protein, A/T-rich interacting domain 3B (ARID3B),  
129 whose expression was enhanced by RTA and that regulated the KSHV lytic cycle. ARID3B, so called  
130 as it contains an A/T-rich interactive domain (ARID), belongs to a family of proteins involved in  
131 the regulation of gene expression. The ARID of ARID3A (a paralogue of ARID3B that functions as  
132 a B cell activator) has been shown to preferentially bind AATTAA sequences (41, 42); as this  
133 domain shares 89.9% sequence identity with that found in ARID3B, it suggests there is functional  
134 conservation between these proteins.

135 As a transcription factor (43, 44), ARID3B promotes survival during development (44-46), and it  
136 is these properties that link it with various malignancies (43, 47-52). Very little else is known  
137 about ARID3B; however, we reasoned that its prosurvival properties may be important during  
138 the KSHV lytic cycle and it might promote lytic gene expression, thus explaining its RTA-mediated  
139 enhanced expression. However, we found that ARID3B inhibited lytic reactivation, and, as it  
140 preferentially bound to regions containing A/T-rich elements in oriLyt, we consider the possibility  
141 that it either prevents oriLyt-dependent gene expression or it blocks access to proteins essential  
142 for viral genome replication.

143 **Materials and Methods**

144 **Cell lines, plasmids and transfections.** TREx-BCBL-1-RTA cells (a kind gift from Dr. Jae Jung,  
145 University of Southern California) are a BCBL-1-based cell line that has been engineered to  
146 inducibly express exogenous Myc-tagged RTA by the addition of 1 µg/ml doxycycline hyclate,  
147 leading to a robust reactivation of the full KSHV lytic cycle (53); these were cultured in RPMI-1640  
148 (Lonza) supplemented with 10% FBS (Life Technologies). Inducible SLK-BAC16 cells (iSLK-BAC16;  
149 also a gift from Dr. Jae Jung) were grown in DMEM (Lonza) supplemented with 10% FBS (Life  
150 Technologies). These maintain a latent infection with bacterial artificial chromosome 16-  
151 (BAC16)-derived KSHV (54). The parental SLK cell line, originally considered to be KSHV-negative  
152 endothelial cells derived from a KS patient, were subsequently found to be a contaminant of a  
153 renal carcinoma cell line Caki1 (55). Nevertheless, they are widely used as a model for the study  
154 of KSHV biology. Initially, these cells were engineered to inducibly express RTA (iSLK) following  
155 the addition of doxycycline (56) and subsequently transfected with BAC16 and selected based on  
156 BAC-derived puromycin resistance (54). This cell line was demonstrated to support an authentic  
157 latent infection, and induction of the lytic cycle (with 1 µg/ml doxycycline hyclate) leads to the  
158 release of infectious virus (54).

159 HEK 293T cells were used for reinfection assays as previously described (57). HEK293 rKSHV.219  
160 cells (58) maintains KSHV as a latent infection and was generated by infecting HEK293T cells with  
161 a recombinant KSHV that contains a constitutively active puromycin resistance and GFP gene,  
162 and an RFP gene that is fused to an RTA-responsive lytic cycle (*PAN*) promoter (not utilized in this

163 study). Both HEK 293T-based cell lines were maintained in DMEM (Lonza) supplemented with 10%  
164 FBS (Life Technologies).

165 To generate cells with inducible N-terminal FLAG-His-tagged RTA expression (iRTA-293), RTA was  
166 amplified from pRTS-ORF50 (14) (forward primer: 5'-  
167 ATCTTAAGGCCACCATGGATTATAAAGATGACGATGACAAGCATCATCATCATCATGCGCAAGATG  
168 ACAAGGGTAAG-3', reverse primer: 5'-ATCTCGAGTCAGTCTCGGAAGTAATTACG-3') and ligated in  
169 to the *AflI-XhoI* sites of pcDNA5-FRT-TO (Life Technologies) to generate pcDNA5-FH-RTA.  
170 Functionality of this vector was demonstrated due to its ability to reactivate the KSHV lytic cycle  
171 following its transfection. Flp-In-293 cells (Life Technologies) were transfected along with pOG44  
172 (flp recombinase) and subsequently selected using Hygromycin B following the manufacturer's  
173 protocol (Life Technologies). Clonal populations were generated by limiting dilution under  
174 Hygromycin B selection and clones with tightly regulated expression and normal growth  
175 properties (compared to parental cells) were selected. RTA expression was induced following  
176 treatment with 1 µg/ml doxycycline hyclate for the indicated times. iRTA-293 cells were  
177 maintained in DMEM (Lonza) supplemented with 10% FBS (Life Technologies).

178 The vector expressing C-terminally FLAG-tagged ARID3B was generated by PCR amplification  
179 using an ARID3B-containing plasmid (kind gift from Dr. Karen Cowden Dahl, Indiana University)  
180 as template (Forward primer: 5'-CGCGGATCCAAGCGATGGAGCCACTTCAGCAGCAGCAGCA-3',  
181 reverse primer: 5'-  
182 CGCGAATTCTCACTTATCGTCGTCATCCTTGTAAATCGAGGGACCAGCTGGTGGAGGGCTC-3'). Products  
183 were digested and ligated into the *Bam*HI and *Eco*RI sites of pcDNA3 (pcDNA3-ARID3B-FLAG).

184 FLAG-tagged SRAG was a kind gift from Prof Stuart Wilson (University of Sheffield). Expression  
185 constructs were verified by DNA sequencing.

186 For transfections, cells were plated into 6-well plates and transfections routinely used 1 µg  
187 plasmid DNA and Lipofectamine 2000 (Life Technologies) following the manufacturer's  
188 instructions.

189 To determine the effects of overexpressed proteins on virus reactivation efficiencies, iSLK-BAC16  
190 cells were transfected for 24 h and the lytic cycle was induced by doxycycline treatment for a  
191 further 24 h. Samples were processed for immunoblot analysis (see later).

192 **Stable isotope labelling of amino acids in cell culture (SILAC)-proteomics.** iRTA-293 cells were  
193 grown in "heavy"-labeled media containing stable isotopes of arginine (R) and lysine (K) (R10K8;  
194 DMEM-16, Dundee Cell Products) or "light"-labeled media (R0K0; DMEM-14, Dundee Cell  
195 Products) supplemented with 10% dialysed FCS (DS1003, Dundee Cell Products) for two weeks.  
196 Cells were grown to 80-90% confluency in 10 cm dishes that included poly-L-lysine coated  
197 coverslips, used to verify RTA expression by immunofluorescence (see later). RTA expression was  
198 induced for 12 h following treatment of heavy-labeled cells with 1 µg/ml doxycycline hyclate. To  
199 reduce sample complexity, and to investigate how RTA expression impacts on the nuclear  
200 proteome, labeled cells were fractionated (verified by immunoblotting; see later). After rinsing  
201 the monolayer with PBS,  $1 \times 10^7$  cells from each culture were lysed in 5 ml cytoplasmic lysis buffer  
202 containing 20 mM Tris (pH 7.4), 100 mM NaCl, 0.5 mM EDTA, 0.5 % NP-40 and 1x protease  
203 inhibitor cocktail (Roche) for 20 min at 4°C. The nuclei were pelleted at 2000 xg for 5 min at 4°C  
204 and the cytoplasmic fraction was removed and stored. Nuclei were washed three times in

205 cytoplasmic lysis buffer, then nuclear proteins were extracted using 200  $\mu$ l RIPA buffer by  
206 repeated pipetting and storage on ice for 15 min. Insoluble material was pelleted at 12,000  $xg$   
207 for 10 min and the supernatant was removed.

208 Equal amounts of protein from unlabeled and labeled samples were combined prior to protein  
209 digestion. Briefly, samples were reduced 50 mM DTT 1x NUPAGE LDS loading buffer, and then  
210 separated by one-dimensional SDS-PAGE (4-12% Bis-Tris Novex mini-gel, Life Technologies) and  
211 visualized by colloidal Coomassie staining (Novex, Life Technologies). The entire protein gel lanes  
212 were excised and cut into 10 slices each. Every gel slice was subjected to in-gel digestion with  
213 trypsin overnight at 37°C. The resulting tryptic peptides were extracted by formic acid (1%) and  
214 acetonitrile, lyophilized in a speed vac and resuspended in 1% formic acid. Trypsin-digested  
215 peptides were separated using an Ultimate 3000 RSLC (Thermo Scientific) nanoflow LC system.  
216 On average 0.5  $\mu$ g was loaded with a constant flow of 5  $\mu$ l/min onto an Acclaim PepMap100  
217 nanoViper C18 trap column (100  $\mu$ m inner diameter, 2cm; Thermo Scientific). After trap  
218 enrichment, peptides were eluted onto an Acclaim PepMap RSLC nanoViper, C18 column (75  $\mu$ m,  
219 15 cm; Thermo Scientific) with a linear gradient of 2–40% solvent B (80% acetonitrile with 0.08%  
220 formic acid) over 65 min with a constant flow of 300 nl/min. The HPLC system was coupled to a  
221 linear ion trap Orbitrap hybrid mass spectrometer (LTQ Orbitrap Velos, Thermo Scientific) via a  
222 nano-electrospray ion source (Thermo Scientific). The spray voltage was set to 1.2 kV, and the  
223 temperature of the heated capillary was set to 250°C. Full-scan MS survey spectra ( $m/z$  335–1800)  
224 in profile mode were acquired in the Orbitrap with a resolution of 60,000 after accumulation of  
225 1,000,000 ions. The fifteen most intense peptide ions from the preview scan in the Orbitrap were  
226 fragmented by collision-induced dissociation (normalized collision energy, 35%; activation Q,

227 0.250; and activation time, 10 ms) in the LTQ after the accumulation of 10,000 ions. Maximal  
228 filling times were 1,000 ms for the full scans and 150 ms for the MS/MS scans. Precursor ion  
229 charge state screening was enabled, and all unassigned charge states as well as singly charged  
230 species were rejected. The lock mass option was enabled for survey scans to improve mass  
231 accuracy. Data were acquired using the Xcalibur software. The raw mass spectrometric data files  
232 obtained for each experiment were collated into a single quantitated data set using MaxQuant  
233 (version 1.2.2.5) and the Andromeda search engine software . Enzyme specificity was set to that  
234 of trypsin, allowing for cleavage N-terminal to proline residues and between aspartic acid and  
235 proline residues. Other parameters used were: (i) variable modifications, methionine oxidation,  
236 protein N-acetylation, Gln to pyro-Glu; (ii) fixed modifications, cysteine carbamidomethylation;  
237 (iii) database: target-decoy human MaxQuant (ipi.HUMAN.v3.68); (iv) heavy labels: R10K8; (v)  
238 MS/MS tolerance: FTMS- 10 ppm , ITMS- 0.6 Da; (vi) maximum peptide length, 6; (vii) maximum  
239 missed cleavages, 2; (viii) maximum of labelled amino acids, 3; and (ix) false discovery rate (FDR),  
240 1%. Peptide ratios were calculated for each arginine- and/or lysine-containing peptide as the  
241 peak area of labelled arginine/lysine divided by the peak area of nonlabelled arginine/lysine for  
242 each single-scan mass spectrum. Peptide ratios for all arginine- and lysine-containing peptides  
243 sequenced for each protein were averaged. Data were normalized using 1/median ratio value for  
244 each identified protein group per labelled sample. Pathway analysis was performed using DAVID  
245 Bioinformatics Resources [<https://david.ncifcrf.gov/>] (59, 60) using proteins that were at least 2-  
246 fold differences.

247 **Immunoprecipitation and Immunoblotting.** Immunoprecipitation assays have been described  
248 previously (61). For immunoblot analysis, cells were washed in PBS and proteins extracted in lysis

249 buffer containing 50 mM Tris (pH 7.4), 150 mM NaCl, 1% NP-40 and 1x protease inhibitor cocktail  
250 (Roche) for 15 min on ice and clarified by centrifugation at 12,000 *xg* for 10 min, 4°C. For the  
251 detection of ARID3B by immunoblotting, we found that sonication prior to loading improved  
252 detection. SDS-PAGE and immunoblotting of normalized protein concentrations followed  
253 standard techniques using the following antibodies: rabbit pAb anti-FLAG-tag (1:1000; Sigma),  
254 mouse mAb anti-ORF57 207.6 (1:1000; Santa Cruz), RTA, rabbit antisera (1:400; gift from Prof.  
255 David Blackbourn, University of Surrey), mouse mAb anti-GAPDH (1:5000; Sigma), mouse mAb  
256 anti-Lamin B1 (1:1000; Santa Cruz), rabbit  $\alpha$ ARID3B (1:200; Abcam), anti-ORF59 (Autogen  
257 Bioclear), sheep anti-KSHV minor capsid protein (mCP 1:1000; Exalpha Biologicals, Inc.). Proteins  
258 were detected by chemiluminescence (using HRP-conjugated secondary antibodies) and signals  
259 were captured digitally using the ChemiDoc MP Imager (Bio-Rad) that ensures signal saturation  
260 does not occur. ImageLab software version 4.1 (Bio-Rad) was used to select and determine the  
261 background-subtracted density of the bands in all blots and these were normalized against  
262 expression of GAPDH.

263 **Indirect immunofluorescence microscopy.** As previously described (62), coverslips were coated  
264 with poly-L-lysine and TReX-BCBL-1-RTA cells were plated ( $1 \times 10^6$  per well of a 12-well plate) and  
265 doxycycline hyclate-treated (1  $\mu$ g/ml) for 18 h at 37°C. Following doxycycline hyclate treatment  
266 of SILAC-labeled iRTA-293 cells (see above), coverslips were removed from the 10 cm dishes and  
267 placed in a humidity chamber. Cells were gently washed with PBS, fixed using 4% formaldehyde  
268 (in PBS) for 10 min, permeabilized with PBS, 1% Triton X-100 for 10 min and washed three times  
269 with PBS as previously reported (62). Primary antibodies were diluted in PBS, 2% BSA, added to  
270 cells and incubated in humidity chambers for 2 h at 37°C or overnight at 4°C followed by 5 washed

271 with PBS. The appropriate secondary antibodies (Alexa Fluor 488 or 594; Life Technologies) were  
272 diluted 1:500 in PBS, 2% BSA and incubated with cells for 1 h at 37°C followed by 5 washed with  
273 PBS. Coverslips were mounted in VECTORSHEILD with DAPI (Vectorlabs).

274 Incorporation of EdU was performed using a Click-iT EdU Imaging Kit (Life Technologies) (62).  
275 Briefly,  $1 \times 10^6$  TReX-BCBL-1-RTA cells were treated doxycycline and the cells were plated onto  
276 poly-L-lysine-coated coverslips. After 16 h, cells were pulsed for 45 min with 10  $\mu$ M EdU, washed,  
277 fixed and permeablized according to the manufacturer's recommendations. After detection of  
278 EdU (according to the manufacturer's protocol), the cells were washed and further incubated  
279 with the indicated antibody for 1 h at 37°C, washed again and incubated with Alexa Fluor 488  
280 goat anti-rabbit antibody (Life Technologies; 1:500 in PBS, 2% BSA) for 1 h at 37°C. Finally, DNA  
281 was stained using Hoechst 33342 (1:2000 in PBS) and mounted in VECTORSHIELD (Vectorlabs).  
282 Images were captured using an LSM510 or LSM700 laser scanning microscope (Carl Zeiss) and  
283 processed using ZEN imaging software (Carl Zeiss).

284 Antibodies included: rabbit anti-FLAG (1:250; Sigma), mouse anti-Myc tag 9E10 (1:250; Sigma),  
285 RTA rabbit antisera (1:100), rabbit anti-ARID3B (1:100; Abcam).

286 **Quantitative PCR.** For RT-qPCR, total cellular RNA was extracted from cells using Trizol (Life  
287 Technologies) according to the manufacturer's instructions and contaminating DNA was  
288 removed using the DNA-free kit (Ambion). Complimentary DNA (cDNA) was generated from 1  $\mu$ g  
289 RNA in 20  $\mu$ l reaction volumes using M-MuLV reverse transcriptase (RT; New England Biolabs)  
290 according to the manufacturer's recommendations with 5 ng oligo(dT). In parallel, negative  
291 control reactions were performed for each RNA by omitting RT in order to confirm that

292 quantification represented cDNA and not contaminating DNA. For quantification of viral DNA,  
293  $1 \times 10^6$  cells were treated with doxycycline hyclate, or left untreated. At 72 h post-reactivation,  
294 total DNA was extracted using a DNA Minikit (Qiagen) and quantified by UV spectrophotometry.  
295 Viral DNA was quantified using primers specific for the ORF57 gene. Quantitative PCR reaction  
296 mixes (20  $\mu$ l) included 1x SensiMix SYBR green master mix (Bioline), 0.5  $\mu$ M each primer and 1  $\mu$ l  
297 cDNA or 3.4 ng total DNA. Cycling was performed in a RotorGene Q machine (Eppendorf) and  
298 included an initial 10 min denaturation step at 94°C, followed by 40 cycles of 30 s at 94°C, 30 s at  
299 60°C and 30 s at 72°C. Melting curve analysis was performed between 65 and 95°C (with 0.2°C  
300 increments) to verify amplicon specificity. Quantification of *GAPDH* mRNA (qRT-PCR) or GAPDH  
301 DNA (virus reactivation) was used to normalize between samples, and the average cycle  
302 threshold (CT) was determined from three independent samples from independent cultures.  
303 Calculations were made using the  $\Delta\Delta$ CT method.

304 **RNAi.** Conditions for siRNA knockdown of ARID3B followed previously reported protocols (57).  
305 Briefly, 20 nM of SMARTpool: ON-TARGETplus ARID3B siRNA (L-012219-00-0005, Dharmcon) or  
306 Hs\_ARID3B\_3 FlexiTube GeneSolution (GS10620, Qiagen), or scramble control siRNA (siRNA  
307 controls from the respective manufacturer were used as controls), were transfected into iSLK-  
308 BAC16 cells for 72 h. For experiments that required reactivation of the lytic cycle, doxycycline  
309 was added to cells for 24 h, as stated above.

310 ***In vitro* DNA affinity assay.** Assays were performed according to (25), with minor modifications:  
311 HEK293 rKSHV.219 cells in 6-well plates were transfected with pcDNA3-ARID3B-FLAG and the  
312 lytic cycle was induced for 24 h. OriLyt sequences 3F, 9F and 11F were amplified from the KSHV

313 genome using 5'-Biotinylated primers (primer sequences already described (25)) and a control  
314 region of the KSHV genome (RTA gene body: forward primer 5'-GTCTACCTTCCGAGGATTATGG-3',  
315 reverse primer : 5'-GATTCTGGCATGAGACCGCTTC-3'). PCR products were incubated with  
316 Dynabeads M-280 Streptavidin according to the manufacturer's recommendations (Life  
317 Technologies). Affinity purification followed the previously described methods (25).

318 **Chromatin immunoprecipitation.** Cells were cross-linked with 1% formaldehyde (Thermo  
319 Scientific, no. 28908) for 10 min at room temperature. Glycine was added to a final concentration  
320 of 125 mM to stop the cross-linking reaction, and the samples were incubated for another 5 min  
321 at room temperature. Cells were washed twice with ice-cold PBS and lysed in FastChIP buffer (50  
322 mM Tris-HCl [pH 7.5], 150 mM NaCl, 5 mM EDTA, 0.5 mM DTT, 0.5% Igepal CA-630, 1.0% Triton  
323 X-100) containing protease inhibitors (Roche) as described (63, 64). Isolated nuclei were  
324 resuspended in SDS lysis buffer (50 mM Tris-HCl [pH 8.1], 10 mM EDTA, 1% SDS) and the samples  
325 were incubated on ice for 15 min. Nuclear lysates were sonicated for 10 min in a Diagenode  
326 Bioruptor Pico (30 sec on-off intervals) and cleared by centrifugation for 30 min at 20,000×g and  
327 4°C. Sheared chromatin from 9×10<sup>6</sup> cells (180µl) was combined with nine volumes of CHIP dilution  
328 buffer (16.7 mM Tris-HCl [pH 8.1], 167 mM NaCl, 1.2 mM EDTA, 1.1% Triton X-100, 0.01% SDS)  
329 and subjected to immunoprecipitation for 16 h at 4°C with gentle rotation using 13 µl of Rabbit  
330 anti-ARID3B antibody (Bethyl Laboratories, no. A302-564A-M) or 4 µg of normal rabbit IgG.  
331 Samples were centrifuged for 10 min at 20,000×g, 4°C to remove any precipitated material, and  
332 the supernatants were combined with 20 µl Magna CHIP Protein A Magnetic Beads (Millipore, no.  
333 16-661) and incubated for 2 h at 4°C with gentle rotation. Immune complexes were washed with  
334 1 ml each of low-salt buffer (20 mM Tris-HCl [pH 8.1], 150 mM NaCl, 2 mM EDTA, 1% Triton X-

335 100, 0.1% SDS), high-salt buffer (20 mM Tris [pH 8.1], 0.5 M NaCl, 2 mM EDTA, 1% Triton X-100,  
336 0.1% SDS), lithium chloride (LiCl) buffer (10 mM Tris [pH 8.1], 0.25 M LiCl, 1 mM EDTA, 1% Igepal-  
337 CA 630, 1% deoxycholic acid), and twice with TE (10 mM Tris-HCl [pH 8.0], 1 mM EDTA) buffer.  
338 Elution of the chromatin-antibody complexes was carried out by incubation with 150 µl freshly  
339 prepared elution buffer (100 mM NaHCO<sub>3</sub>, 1% SDS) containing 1.5 µl Proteinase K (Roche, no. 03  
340 115 887 001) at 62°C for 2 h, followed by a 10 min incubation step at 95°C. DNA was purified  
341 using the NucleoSpin Gel and PCR Clean-up Kit from Macherey-Nagel (no. 740609) following their  
342 DNA clean-up protocol for samples containing SDS. DNA was eluted with 90 µl Buffer NE and 5 µl  
343 of the DNA solution were used as template DNA for qPCR using primers specific for the A/T-rich  
344 region of oriLyt left (forward primer: 5'-CCCTCCTTTGTTTTCCGGAAG-3' and reverse primer:  
345 5'CTCATCGGGCCCTATTATAAAG-3') and the RTA coding region (forward primer 5'-  
346 GTCTACCTCCGAGGATTATGG-3', reverse primer : 5'-GATTCTGGCATGAGACCGCTTC-3').

347

348 **Results**

349 **ARID3B expression is enhanced by RTA.** To investigate the impact of the lytic-switch protein RTA  
350 expression on the host proteome, we developed a cell line with doxycycline-inducible RTA  
351 expression (iRTA-293) and applied global proteomics using stable isotope labeling of amino acids  
352 in cell culture (SILAC). After metabolically labelling cells in media containing different stable  
353 isotopes of arginine (R) and lysine (K) (e.g. R10K8 (heavy) or R0K0 (light)) for two weeks, we  
354 induced RTA expression from heavy-labeled cells for 12 h while leaving light-labeled cells  
355 untreated. We tested RTA expression by immunofluorescence and then fractionated cells into  
356 cytoplasmic and nuclear fractions that were validated by immunoblot analysis using cytoplasmic  
357 and nuclear markers (Fig. 1A-B). Both these assays demonstrated the expected nuclear  
358 expression of RTA. We combined the nuclear fractions (heavy vs. light) 1:1 and applied LC-MS/MS  
359 (Dundee Cell Products, see Materials and Methods). Identified and quantified proteins with a  
360 minimum of two unique peptides and a fold change in abundance of >2-fold were taken forward  
361 for bioinformatics analyses. KEGG pathway analysis of the nuclear proteome of proteins  
362 increased in abundance upon RTA expression (using DAVID Bioinformatics Resources (59, 60))  
363 identified various pathways one might expect to be modulated upon RTA expression (e.g. cell  
364 cycle control (65) and DNA replication (24); (Fig. 1C). However, various DNA damage response  
365 (DDR) pathways were also identified in addition to ubiquitin-mediated proteolysis (specifically  
366 Cullin-RING ubiquitin ligases [CRLs]). A cellular mechanism that regulates CRLs (66-68) and many  
367 of the listed DDR pathways (69-71) is the ubiquitin-like modification NEDDylation. Of note, we  
368 recently showed that blocking NEDDylation in cells latently infected with KSHV resulted in the  
369 activation RTA expression, but inhibited viral DNA replication (62). Interestingly, a similar

370 observation (with regards to effects on viral gene expression and viral DNA replication) was  
371 recently reported for the betaherpesvirus, human cytomegalovirus (HCMV); blocking of  
372 NEDDylation also led to increased immediate early gene expression in the absence of viral DNA  
373 replication (72). Furthermore, both of these reports showed that Cullin 4B was particularly  
374 important for regulating viral gene expression (62, 72).

375 In addition to investigating cellular pathways associated with RTA expression, we compiled a list  
376 of the top 15 proteins that showed increases in abundance in RTA expressing cells (Table 1).  
377 Interestingly, a number of proteins associated with transcriptional repression were identified  
378 (cell division cycle-associated 7-like (15.5-fold increase), Polycomb group protein  
379 Lethal(3)malignant brain tumor-like protein 3 (5.7-fold increase) and lysine-specific demethylase  
380 2A (5.2-fold increase)). We also note that RTA expression was associated with an increased  
381 abundance of protein LYRIC (7.0-fold increase) that has been shown to activate NF- $\kappa$ B (Table 1);  
382 intriguingly, these data suggest that RTA is associated with the expression of factors that one  
383 would predict to inhibit RTA's transcriptional activity. In accordance with this, we also applied  
384 Ingenuity Pathways Analysis (IPA) to the same dataset, and the top canonical pathway identified,  
385 in addition to cell cycle control, DNA replication and various DNA damage pathways, was  
386 'transcriptional repression' (Table 2). We are currently investigating some of these observations  
387 and in this report we focus on the novel protein ARID3B (7.5-fold increase). There are a number  
388 of features that led us to investigate ARID3B. Relatively little is known about this protein, and  
389 using KSHV as a tractable model system, we wished to further study its function. It has been  
390 shown that ARID3B functions as a transcription factor linked with prosurvival mechanisms during  
391 developmental processes (44-46), and these functions may be beneficial for reactivation.

392 Furthermore, ARID domains have been described as DNA binding domains that favor A/T-rich  
393 sequences; given the predominance of A/T-rich elements in regulatory regions of the KSHV  
394 genome (RREs, oriLyt etc.), we hypothesized that ARID3B would cooperate with RTA during  
395 reactivation of the lytic cycle.

396 To investigate how RTA expression might lead to an increase in ARID3B levels, we induced RTA  
397 expression in iRTA-293 cells in addition to reactivating the lytic cycle in TReX-BCBL-1-RTA cells  
398 (see Materials and Methods for a description of the cell lines used in this study). We performed  
399 RT-qPCR analysis and found that RTA, and lytic reactivation, led to a small but reproducible  
400 increase in *ARID3B* mRNA expression (ca. 2.5-fold increase, Fig. 2A). We also reactivated the lytic  
401 cycle in iSLK-BAC16 and TReX-BCBL-1-RTA cells and performed immunoblot analyses using  
402 antibodies specific for ARID3B (Fig. 2B). This showed that lytic reactivation led to an approximate  
403 1.5 - 2-fold increase in ARID3B expression (Fig. 2C). These changes are modest, but likely reflect  
404 the superior sensitivity of mass spectrometry, and the semi-quantitative nature of immunoblot  
405 data. Together, these data demonstrate that RTA, and the KSHV lytic cycle, enhances ARID3B  
406 expression at both the RNA and protein level.

407 **ARID3B is relocalized during reactivation.** Given that ARID3B expression levels were influenced  
408 by RTA expression and lytic reactivation, we next asked whether it was involved in regulating the  
409 KSHV lytic cycle. Using an immunofluorescence microscopy approach, we showed that in latently  
410 infected TReX-BCBL-1-RTA cells, ARID3B expression displayed a pan-nuclear (excluding nucleoli)  
411 localization (Fig. 3A; -Dox. (latent)). However, upon lytic reactivation, ARID3B is relocalized to  
412 discrete, RTA-positive foci, with close proximity to the nuclear periphery (Fig. 3A; +Dox. (lytic),

413 compare the RTA-positive, reactivated cells to the RTA-negative cell in the same field of view),  
414 reminiscent of replication compartments (also known as replication and transcription  
415 compartments, RTCs). Replication compartments are distinct, RTA-positive foci found at the  
416 nuclear periphery associated with newly replicated viral DNA (that are observed via incorporation  
417 of BrdU or EdU that specifically marks viral DNA due to KSHV's ability to block cellular DNA  
418 replication during reactivation). We performed an independent experiment to ask if ARID3B did  
419 indeed relocalize to these foci. Consequently, ARID3B was again shown to co-stain with RTA and  
420 to colocalize with EdU-positive foci (Fig. 3B) suggesting that it did indeed relocalized from a pan-  
421 nuclear pattern into KSHV replication compartments upon lytic reactivation.

422 **ARID3B modulates the KSHV lytic cycle.** To investigate if ARID3B influenced the KSHV lytic cycle,  
423 we transfected iSLK-BAC16 cells with two separate pools of *ARID3B*-targeted or scramble control  
424 siRNAs and induced the lytic cycle with doxycycline for 24 h. Given that ARID3B has been  
425 suggested to function as a transcription factor, we anticipated that it might be important for  
426 enhancing RTA-mediated expression of lytic genes. Using RT-qPCR we demonstrated an  
427 approximately 50% knockdown of *ARID3B*. This was sufficient to enhance lytic gene expression  
428 between 1.5 – 2.5-fold, as shown for lytic genes *ORF57* and *gB* (Fig. 4A), suggesting that ARID3B  
429 might actually inhibit lytic gene expression. We noticed that the two siRNAs had slightly different  
430 effects on lytic gene expression; these two siRNA preparations were mixtures of three different  
431 sequences, and it might be that one of these more potently targets *ARID3B*. However, we cannot  
432 fully explain this as the current time, and this difference was not observed in other assays with  
433 this set of siRNAs. ARID3B knockdown was also associated with an approximate 2-fold increase  
434 in lytic protein expression (Fig. 4B-C). Accordingly, ARID3B knockdown, followed by reactivation

435 of the lytic cycle, also led to a significant enhancement of KSHV genome replication compared to  
436 cells transfected with a scramble control siRNA (Fig. 4D). Importantly, knockdown in latently  
437 infected cells did not activate viral DNA replication (Fig. 4D) suggesting that RTA expression, or  
438 the lytic cycle were required to activate ARID3B's inhibitory properties.

439 To ask if the increases in lytic cycle-associated expression and genome replication led to an  
440 enhanced productive infection, we harvested and clarified media from iSLK-BAC16 cells that had  
441 been transfected with ARID3B siRNA and reactivated with doxycycline. We transferred this media  
442 to KSHV-negative cells (HEK 293T), and 24 h later, purified total cellular RNA. Using RT-qPCR  
443 analysis of the KSHV *ORF57* gene as a measure of virus infection, we demonstrated knockdown  
444 of ARID3B led to an enhancement of virus infection, suggesting that ARID3B knockdown led to  
445 an increase of released virions (Fig. 4E). Together, these data showed that ARID3B knockdown  
446 enhanced the KSHV lytic cycle, contrary to our initial hypothesis. However, these differences  
447 were modest given our inability to reduce ARID3B expression more than 50-60%. Therefore, we  
448 took an alternative approach and asked if ARID3B overexpression could inhibit KSHV reactivation.  
449 Here we showed that transfection of FLAG-tagged ARID3B, but not FLAG-SRAG (used as a control  
450 as we know its expression does not modulate lytic reactivation), in iSLK-BAC16 cells for 24 h,  
451 followed by reactivation of the lytic cycle, inhibited the expression of KSHV lytic genes (Fig. 4F).  
452 Together, these data demonstrate that ARID3B is able to modulate KSHV reactivation, and not  
453 enhance it, as originally predicted.

454

455 **ARID3B interacts with an A/T-rich region of ori<sub>Lyt</sub> in a lytic reactivation-dependent manner.** To  
456 investigate a potential mechanism whereby ARID3B tempered KSHV lytic reactivation, we tested

457 the possibility that ARID3B interacted with RTA and inhibited its function. RTA interacts with  
458 various cellular proteins that are known to be inhibitory, including PARP1 (34), TLE2 (33) and  
459 HDAC1 (35). However, co-immunoprecipitation assays demonstrated that while RTA interacted  
460 with a known binding partner ORF59 (22), it did not interact with ARID3B (Fig. 5). Next, we  
461 reasoned that ARID3B, as a DNA binding protein, might interact with viral genomes. Furthermore,  
462 due to its predicted preference for A/T-rich sequences, and the existence of these sequences in  
463 oriLyt, we focused our attention to this region of the KSHV genome. We performed a DNA affinity  
464 assay that has previously been reported as a method for identifying proteins involved in KSHV  
465 reactivation (25). Biotinylated PCR products that spanned oriLyt were amplified from KSHV DNA  
466 (Fig. 6A) were bound to streptavidin-coated beads and incubated with lysate from reactivated  
467 HEK293T-rKSHV.219 cells that had been transfected with FLAG-ARID3B 24 h earlier. Compared  
468 to control DNA (amplified from the RTA coding region), and a central G/C-rich repeat region (“9F”)  
469 we found that ARID3B preferentially bound to “3F” which contains the A/T-rich region of KSHV  
470 oriLyt (Fig. 6A). ARID3B also bound to “11F” which contained the RTA-responsive element (RRE),  
471 although this appeared to be slightly reduced when compared to the 3F region. Interestingly, it  
472 was shown previously that many host and viral proteins involved in KSHV reactivation specifically  
473 bind these two regions in oriLyt (25).

474 We confirmed this result using chromatin immunoprecipitation (ChIP) assays using TReX-BCBL-  
475 1-RTA cells. This allowed to us investigate whether ARID3B interacted with the KSHV genome in  
476 infected cells, in addition to asking if this was linked with reactivation of the lytic cycle. Using an  
477 antibody that has previously used in ChIP assays (43), we showed that endogenous ARID3B  
478 interacted preferentially with the A/T-rich region of oriLyt (3.5-fold enrichment over control IgG

479 antibody), and not within the RTA gene (Fig. 6B). Furthermore, we showed that this interaction  
480 was dependent on reactivation of the KSHV lytic cycle as no binding (above control IgG antibody)  
481 was observed in latent cells (Fig. 6B). These data, together with data in Fig. 2 (lytic cycle-  
482 associated relocalization) and Fig. 4 (knockdown of ARID3B does not induce viral DNA replication),  
483 suggest that ARID3B influences KSHV biology only upon reactivation of the lytic cycle.

484

485 **Discussion.**

486 It is well established that KSHV is the etiologic agent of various malignancies in immune-  
487 compromised individuals, particularly those infected with HIV. Indeed, KS is the most prevalent  
488 malignancy in regions with endemic HIV and, for HIV sufferers, is one of a number of diseases  
489 that are used as a guideline for the diagnosis of AIDS (i.e. KS is considered an AIDS-defining  
490 disease) (2). Importantly, various reports, including data from clinical studies, link reactivation of  
491 the KSHV lytic cycle with the pathogenesis of KS. Therefore, it is imperative that we understand  
492 the mechanisms that regulate this aspect of KSHV biology. RTA, the KSHV lytic switch protein, is  
493 both necessary and sufficient for reactivation of the lytic cycle (8). While we have a relatively  
494 good understanding of how RTA drives the viral transcriptional program responsible for lytic  
495 reactivation (8), how RTA influences cellular responses is less well understood. In this report we  
496 developed a cell line with inducible RTA expression and, by applying a quantitative proteomics  
497 approach, used it to investigate what impact RTA expression has on the cellular proteome.

498 We identified a number of cellular pathways that were associated with RTA expression, and some  
499 of these are the focus of current research. Of note, ubiquitin-mediated proteolysis was one of  
500 the gene ontology terms included in our bioinformatics analyses. We, and others, have recently  
501 reported the importance of this pathways for regulating herpesvirus gene expression, and  
502 demonstrated that this pathway represents a potential therapeutic target for the treatment of  
503 herpesvirus disease (62, 72). In addition to studying cellular pathways, we generated a list of the  
504 top 15 proteins based on increased protein abundance in RTA-expressing cells. In this report, we  
505 focused on a little-known protein ARID3B. We initially hypothesized that, as a prosurvival

506 transcription factor (43, 44), this protein would cooperate with RTA during reactivation of the  
507 lytic cycle. However, we actually found that ARID3B played an inhibitory role, and its expression  
508 was associated with modulating lytic reactivation.

509 A hallmark of all herpesviruses is their ability to establish a latent infection characterized by a  
510 highly restricted gene expression program. This is an incredibly effective means of evading  
511 detection by the immune system, and ensures infection is maintained throughout the life of the  
512 host. Nevertheless, periodic reactivation of the lytic cycle is necessary in order to maintain the  
513 population of infected cells. However, the lytic cycle must be exquisitely regulated so that it does  
514 not lead to uncontrolled virion production and severe disease in its host. We observed that upon  
515 RTA expression, or reactivation of the lytic cycle, ARID3B expression was increased both at the  
516 mRNA and protein level. To ascertain if this had functional consequences for KSHV reactivation,  
517 we performed a series of experiments that showed ARID3B was able to block reactivation. This  
518 included siRNA-mediated knockdown of ARID3B, which resulted in enhanced lytic gene  
519 expression, lytic protein expression and an increase in genome replication. Furthermore,  
520 knockdown of ARID3B potentially led to an increase in virion production, as suggested by  
521 reinfection assays. As an alternative approach, overexpression of ARID3B significantly abrogated  
522 lytic protein expression. Importantly, knockdown of ARID3B in latently infected cells did not  
523 reactivate the lytic cycle, suggesting that it was not involved in the maintenance of latency.  
524 Therefore, RTA-mediated activation of ARID3B specifically served to regulate lytic reactivation;  
525 however, it is also possible that this inhibitory function may be important during the  
526 establishment phase of latency.

527 KSHV reactivation leads to the upregulation of several negative feedback processes that temper  
528 the lytic cycle, many of which center on abrogating RTA's interaction with RBP-Jk (required for  
529 transactivating various lytic gene promoters via the 'indirect' mechanism (8)). For example, and  
530 in a similar vein to the observed RTA-enhanced ARID3B expression, RTA enhances the expression  
531 of the co-repressor transducin-like enhancer of split 2 (TLE2) that blocked lytic reactivation by  
532 competing with RBP-Jk for the same binding site in RTA (33) (we did not identify TLE2 in our  
533 datasets). Lytic reactivation also promotes nuclear translocation of the transcription factor NF-  
534  $\kappa$ B, which in turn negatively regulates lytic cycle-associated gene expression by competing with  
535 RTA for RBP-Jk binding (32, 73, 74). Furthermore, activated NF- $\kappa$ B is required for the expression  
536 of latency-associated genes (e.g. *LANA*, *vFLIP*, *vCyclin*), and *LANA* has been shown to inhibit lytic  
537 reactivation, again, by interfering with RTA-RBP-Jk interactions (75, 76). Additional negative  
538 regulatory mechanisms involve RTA interactions with histone deacetylase enzymes HDAC1 (35)  
539 and SIRT1 (77), which limits RTA's ability to activate lytic gene transcription. We do not currently  
540 know how RTA led to increases in ARID3B expression. As a transcription factor, RTA may drive  
541 the expression of *ARID3B*; it may also be possible that RTA induces ARID3B expression indirectly.  
542 Here, two possibilities exist: i) RTA expression may promote a cellular response that is linked to  
543 ARID3B expression or ii) RTA may sequester a repressor that would normally silence *ARID3B*. As  
544 there are no reports describing the regulation of ARID3B expression, it is not possible to go  
545 beyond speculation.

546 Commencement of the lytic cycle leads to a dramatic remodelling of the cell nucleus and the  
547 formation of discrete foci (termed replication compartments) where viral transcription, genome  
548 replication and capsid assembly takes place (78). For KSHV, the formation of replication

549 compartment was recently shown to be dependent on the chaperone function of Hsp70 proteins  
550 (57). We observed that, upon lytic reactivation, ARID3B relocalized from a pan-nuclear pattern,  
551 to replication compartments as shown by its colocalization with RTA and EdU. Of note, it was also  
552 recently shown that lytic reactivation induced the relocalization of TLE2 in to replication  
553 compartments (33), highlighting a common feature among negative regulators of the lytic cycle.  
554 This suggested that ARID3B might inhibit reactivation by interacting with a protein required for  
555 lytic reactivation (cellular or viral), or the viral genome, although these scenarios are not  
556 necessarily mutually exclusive. Interestingly, RTA and ARID3B did not interact. This was  
557 somewhat surprising; however, as a DNA binding protein, an interaction with RTA may not be  
558 necessary for it to associate with reactivated KSHV. Therefore, unlike the majority of lytic cycle  
559 regulators that have been shown to interact directly with RTA, ARID3B performs this task via a  
560 different mechanism.

561 We reasoned that ARID3B, as a DNA binding protein, might interact with viral genomes.  
562 Particularly, given its proposed preference for A/T-rich sequences and the presence of these  
563 sequences in oriLyt, we considered the possibility that ARID3B binds to this region of the genome.  
564 Indeed, DNA affinity (Fig. 6A) and ChIP assays (Fig. 6B) demonstrated that this was the case. The  
565 DNA affinity assay showed us that overexpressed ARID3B preferentially bound to a region of  
566 oriLyt that also contains A/T-rich palindromic sequences in addition to a downstream region  
567 which contained the RTA-responsive element (RRE). Interestingly, it was previously shown that  
568 many host and viral proteins involved in KSHV reactivation specifically bind these two regions in  
569 oriLyt (25).

570 Importantly, CHIP assays not only allowed us to confirm binding *in vivo*, it also allowed us to ask  
571 if its interaction was dependent on lytic reactivation. This was an important question as much of  
572 our data suggested that ARID3B's inhibitory properties were associated with RTA expression,  
573 which is silenced during latency; for example, and as mentioned earlier, knockdown of ARID3B  
574 from latently-infected cells did not appear to stimulate lytic gene expression (suggesting it does  
575 not have a role in the maintenance of latency). Strikingly, this interaction was indeed dependent  
576 on reactivation of the lytic cycle, as no binding was observed on the latent genome. This might  
577 suggest that the chromatinized latent KSHV genome precludes ARID3B access; however, upon  
578 reactivation, which is associated with removal of nucleosomes, ARID3B can bind. However, it is  
579 not currently known if ARID3B binding is dependent on chromatin status of DNA. Additionally,  
580 whether this is dependent on direct DNA binding or it requires PPIs, and if ARID3B blocks  
581 transcription or DNA replication are still open questions. Nevertheless, this data provides weight  
582 to the hypothesis that ARID3B specifically responds to reactivation of the lytic cycle from latency  
583 and inhibits it via interactions with the KSHV genome. We propose that this interaction likely  
584 competes with oriLyt-associated factors required for reactivation of the lytic cycle (Fig. 7).

585 We were surprised to observe that RTA expression induced a number of proteins and pathways  
586 associated with transcriptional silencing (Tables 1 and 2). Although it will be critical to validate  
587 these observations, this might not be surprising given that *de novo* KSHV infection of tissue  
588 culture cells leads to viral latency, despite an initial burst of lytic cycle-associated gene expression  
589 (79). Therefore, while RTA drives expression from the viral genome during reactivation, it may  
590 also induce a number of processes (directly or indirectly) that ultimately silences lytic gene  
591 expression.

592 In summary, we have identified a novel cellular protein, ARID3B, which responds to the lytic cycle  
593 of KSHV, and functions to inhibit it. Lytic cycle-associated induction of negative feedback  
594 mechanisms is clearly an important feature of herpesvirus biology and is consistent with a virus  
595 that favors lifelong infection of its host.

596

### 597 **Acknowledgments**

598 The authors would like to thank Dr Karen Cowden Dahl (University of Notre Dame) and Prof Stuart  
599 Wilson (University of Sheffield) for providing plasmid DNA, Dr Jae Jung (University of Southern  
600 California) for cells and Prof David Blackbourn (University of Surrey) for RTA antisera. We also  
601 thank the Leeds University Bioimaging Facility and Jill McVee (University of St. Andrews) for  
602 assistance with confocal microscopy and Christopher Simmons-Riach (University of St Andrews)  
603 for excellent technical assistance.

604

605 **References.**

- 606 1. **Dittmer DP, Damania B.** 2013. Kaposi sarcoma associated herpesvirus pathogenesis (KSHV)--an  
607 update. *Curr Opin Virol* **3**:238-244.
- 608 2. **Mesri EA, Cesarman E, Boshoff C.** 2010. Kaposi's sarcoma and its associated herpesvirus. *Nat Rev*  
609 *Cancer* **10**:707-719.
- 610 3. **Godfrey A, Anderson J, Papanastasiou A, Takeuchi Y, Boshoff C.** 2005. Inhibiting primary effusion  
611 lymphoma by lentiviral vectors encoding short hairpin RNA. *Blood* **105**:2510-2518.
- 612 4. **Ambroziak JA, Blackbourn DJ, Herndier BG, Glogau RG, Gullett JH, McDonald AR, Lennette ET,**  
613 **Levy JA.** 1995. Herpes-like sequences in HIV-infected and uninfected Kaposi's sarcoma patients.  
614 *Science* **268**:582-583.
- 615 5. **Quinlivan EB, Zhang C, Stewart PW, Komoltri C, Davis MG, Wehbie RS.** 2002. Elevated virus loads  
616 of Kaposi's sarcoma-associated human herpesvirus 8 predict Kaposi's sarcoma disease  
617 progression, but elevated levels of human immunodeficiency virus type 1 do not. *J Infect Dis*  
618 **185**:1736-1744.
- 619 6. **Campbell TB, Borok M, Gwanzura L, MaWhinney S, White IE, Ndemera B, Gudza I, Fitzpatrick L,**  
620 **Schooley RT.** 2000. Relationship of human herpesvirus 8 peripheral blood virus load and Kaposi's  
621 sarcoma clinical stage. *AIDS* **14**:2109-2116.
- 622 7. **Martin DF, Kuppermann BD, Wolitz RA, Palestine AG, Li H, Robinson CA.** 1999. Oral ganciclovir  
623 for patients with cytomegalovirus retinitis treated with a ganciclovir implant. Roche Ganciclovir  
624 Study Group. *N Engl J Med* **340**:1063-1070.
- 625 8. **Guito J, Lukac DM.** 2012. KSHV Rta Promoter Specification and Viral Reactivation. *Front Microbiol*  
626 **3**:30.
- 627 9. **Dalton-Griffin L, Wilson SJ, Kellam P.** 2009. X-box binding protein 1 contributes to induction of  
628 the Kaposi's sarcoma-associated herpesvirus lytic cycle under hypoxic conditions. *J Virol* **83**:7202-  
629 7209.
- 630 10. **Yu F, Feng J, Harada JN, Chanda SK, Kenney SC, Sun R.** 2007. B cell terminal differentiation factor  
631 XBP-1 induces reactivation of Kaposi's sarcoma-associated herpesvirus. *FEBS Lett* **581**:3485-3488.
- 632 11. **Davis DA, Rinderknecht AS, Zoetewij JP, Aoki Y, Read-Connoles EL, Tosato G, Blauvelt A,**  
633 **Yarchoan R.** 2001. Hypoxia induces lytic replication of Kaposi sarcoma-associated herpesvirus.  
634 *Blood* **97**:3244-3250.
- 635 12. **Bu W, Carroll KD, Palmeri D, Lukac DM.** 2007. Kaposi's sarcoma-associated herpesvirus/human  
636 herpesvirus 8 ORF50/Rta lytic switch protein functions as a tetramer. *J Virol* **81**:5788-5806.
- 637 13. **Tsai WH, Wang PW, Lin SY, Wu IL, Ko YC, Chen YL, Li M, Lin SF.** 2012. Ser-634 and Ser-636 of  
638 Kaposi's Sarcoma-Associated Herpesvirus RTA are Involved in Transactivation and are Potential  
639 Cdk9 Phosphorylation Sites. *Front Microbiol* **3**:60.
- 640 14. **Sun R, Lin SF, Gradoville L, Yuan Y, Zhu F, Miller G.** 1998. A viral gene that activates lytic cycle  
641 expression of Kaposi's sarcoma-associated herpesvirus. *Proc Natl Acad Sci U S A* **95**:10866-10871.
- 642 15. **Chang PJ, Shedd D, Miller G.** 2005. Two subclasses of Kaposi's sarcoma-associated herpesvirus  
643 lytic cycle promoters distinguished by open reading frame 50 mutant proteins that are deficient  
644 in binding to DNA. *J Virol* **79**:8750-8763.
- 645 16. **Song MJ, Brown HJ, Wu TT, Sun R.** 2001. Transcription activation of polyadenylated nuclear rna  
646 by rta in human herpesvirus 8/Kaposi's sarcoma-associated herpesvirus. *J Virol* **75**:3129-3140.
- 647 17. **Chang PJ, Shedd D, Gradoville L, Cho MS, Chen LW, Chang J, Miller G.** 2002. Open reading frame  
648 50 protein of Kaposi's sarcoma-associated herpesvirus directly activates the viral PAN and K12  
649 genes by binding to related response elements. *J Virol* **76**:3168-3178.

- 650 18. **Zhang J, Wang J, Wood C, Xu D, Zhang L.** 2005. Kaposi's sarcoma-associated herpesvirus/human  
651 herpesvirus 8 replication and transcription activator regulates viral and cellular genes via  
652 interferon-stimulated response elements. *J Virol* **79**:5640-5652.
- 653 19. **Liang Y, Ganem D.** 2003. Lytic but not latent infection by Kaposi's sarcoma-associated herpesvirus  
654 requires host CSL protein, the mediator of Notch signaling. *Proc Natl Acad Sci U S A* **100**:8490-  
655 8495.
- 656 20. **Matsumura S, Fujita Y, Gomez E, Tanese N, Wilson AC.** 2005. Activation of the Kaposi's sarcoma-  
657 associated herpesvirus major latency locus by the lytic switch protein RTA (ORF50). *J Virol*  
658 **79**:8493-8505.
- 659 21. **Palmeri D, Carroll KD, Gonzalez-Lopez O, Lukac DM.** 2011. Kaposi's sarcoma-associated  
660 herpesvirus Rta tetramers make high-affinity interactions with repetitive DNA elements in the  
661 Mta promoter to stimulate DNA binding of RBP-Jk/CSL. *J Virol* **85**:11901-11915.
- 662 22. **Rossetto CC, Susilarini NK, Pari GS.** 2011. Interaction of Kaposi's sarcoma-associated herpesvirus  
663 ORF59 with oriLyt is dependent on binding with K-Rta. *J Virol* **85**:3833-3841.
- 664 23. **Wang Y, Li H, Chan MY, Zhu FX, Lukac DM, Yuan Y.** 2004. Kaposi's sarcoma-associated herpesvirus  
665 ori-Lyt-dependent DNA replication: cis-acting requirements for replication and ori-Lyt-associated  
666 RNA transcription. *J Virol* **78**:8615-8629.
- 667 24. **Wang Y, Tang Q, Maul GG, Yuan Y.** 2006. Kaposi's sarcoma-associated herpesvirus ori-Lyt-  
668 dependent DNA replication: dual role of replication and transcription activator. *J Virol* **80**:12171-  
669 12186.
- 670 25. **Wang Y, Li H, Tang Q, Maul GG, Yuan Y.** 2008. Kaposi's sarcoma-associated herpesvirus ori-Lyt-  
671 dependent DNA replication: involvement of host cellular factors. *J Virol* **82**:2867-2882.
- 672 26. **Gunther T, Grundhoff A.** 2010. The epigenetic landscape of latent Kaposi sarcoma-associated  
673 herpesvirus genomes. *PLoS Pathog* **6**:e1000935.
- 674 27. **Gunther T, Schreiner S, Dobner T, Tessmer U, Grundhoff A.** 2014. Influence of ND10 components  
675 on epigenetic determinants of early KSHV latency establishment. *PLoS Pathog* **10**:e1004274.
- 676 28. **Toth Z, Maglinte DT, Lee SH, Lee HR, Wong LY, Brulois KF, Lee S, Buckley JD, Laird PW, Marquez  
677 VE, Jung JU.** 2010. Epigenetic analysis of KSHV latent and lytic genomes. *PLoS Pathog* **6**:e1001013.
- 678 29. **Lan K, Kupperts DA, Verma SC, Robertson ES.** 2004. Kaposi's sarcoma-associated herpesvirus-  
679 encoded latency-associated nuclear antigen inhibits lytic replication by targeting Rta: a potential  
680 mechanism for virus-mediated control of latency. *J Virol* **78**:6585-6594.
- 681 30. **Li Q, Zhou F, Ye F, Gao SJ.** 2008. Genetic disruption of KSHV major latent nuclear antigen LANA  
682 enhances viral lytic transcriptional program. *Virology* **379**:234-244.
- 683 31. **Bellare P, Ganem D.** 2009. Regulation of KSHV lytic switch protein expression by a virus-encoded  
684 microRNA: an evolutionary adaptation that fine-tunes lytic reactivation. *Cell Host Microbe* **6**:570-  
685 575.
- 686 32. **Izumiya Y, Izumiya C, Hsia D, Ellison TJ, Luciw PA, Kung HJ.** 2009. NF-kappaB serves as a cellular  
687 sensor of Kaposi's sarcoma-associated herpesvirus latency and negatively regulates K-Rta by  
688 antagonizing the RBP-Jkappa coactivator. *J Virol* **83**:4435-4446.
- 689 33. **He Z, Liu Y, Liang D, Wang Z, Robertson ES, Lan K.** 2010. Cellular corepressor TLE2 inhibits  
690 replication-and-transcription- activator-mediated transactivation and lytic reactivation of  
691 Kaposi's sarcoma-associated herpesvirus. *J Virol* **84**:2047-2062.
- 692 34. **Gwack Y, Nakamura H, Lee SH, Souvlis J, Yustein JT, Gygi S, Kung HJ, Jung JU.** 2003. Poly(ADP-  
693 ribose) polymerase 1 and Ste20-like kinase hKFC act as transcriptional repressors for gamma-2  
694 herpesvirus lytic replication. *Mol Cell Biol* **23**:8282-8294.
- 695 35. **Gwack Y, Byun H, Hwang S, Lim C, Choe J.** 2001. CREB-binding protein and histone deacetylase  
696 regulate the transcriptional activity of Kaposi's sarcoma-associated herpesvirus open reading  
697 frame 50. *J Virol* **75**:1909-1917.

- 698 36. **Griffiths DA, Abdul-Sada H, Knight LM, Jackson BR, Richards K, Prescott EL, Peach AH, Blair GE, Macdonald A, Whitehouse A.** 2013. Merkel cell polyomavirus small T antigen targets the NEMO adaptor protein to disrupt inflammatory signaling. *J Virol* **87**:13853-13867.
- 699
- 700
- 701 37. **Jackson BR, Noerenberg M, Whitehouse A.** 2014. A novel mechanism inducing genome instability in Kaposi's sarcoma-associated herpesvirus infected cells. *PLoS Pathog* **10**:e1004098.
- 702
- 703 38. **Knight LM, Stakaityte G, Wood JJ, Abdul-Sada H, Griffiths DA, Howell GJ, Wheat R, Blair GE, Steven NM, Macdonald A, Blackburn DJ, Whitehouse A.** 2015. Merkel cell polyomavirus small T antigen mediates microtubule destabilization to promote cell motility and migration. *J Virol* **89**:35-47.
- 704
- 705
- 706
- 707 39. **Munday DC, Surtees R, Emmott E, Dove BK, Digard P, Barr JN, Whitehouse A, Matthews D, Hiscox JA.** 2012. Using SILAC and quantitative proteomics to investigate the interactions between viral and host proteomes. *Proteomics* **12**:666-672.
- 708
- 709
- 710 40. **Owen CB, Hughes DJ, Baquero-Perez B, Berndt A, Schumann S, Jackson BR, Whitehouse A.** 2014. Utilising proteomic approaches to understand oncogenic human herpesviruses (Review). *Mol Clin Oncol* **2**:891-903.
- 711
- 712
- 713 41. **Herrscher RF, Kaplan MH, Lelsz DL, Das C, Scheuermann R, Tucker PW.** 1995. The immunoglobulin heavy-chain matrix-associating regions are bound by Bright: a B cell-specific trans-activator that describes a new DNA-binding protein family. *Genes Dev* **9**:3067-3082.
- 714
- 715
- 716 42. **Rhee C, Lee BK, Beck S, Anjum A, Cook KR, Popowski M, Tucker HO, Kim J.** 2014. Arid3a is essential to execution of the first cell fate decision via direct embryonic and extraembryonic transcriptional regulation. *Genes Dev* **28**:2219-2232.
- 717
- 718
- 719 43. **Bobbs A, Gellerman K, Hallas WM, Joseph S, Yang C, Kurkewich J, Cowden Dahl KD.** 2015. ARID3B Directly Regulates Ovarian Cancer Promoting Genes. *PLoS One* **10**:e0131961.
- 720
- 721 44. **Roy L, Samyesudhas SJ, Carrasco M, Li J, Joseph S, Dahl R, Cowden Dahl KD.** 2014. ARID3B increases ovarian tumor burden and is associated with a cancer stem cell gene signature. *Oncotarget* **5**:8355-8366.
- 722
- 723
- 724 45. **Casanova JC, Uribe V, Badia-Careaga C, Giovinazzo G, Torres M, Sanz-Ezquerro JJ.** 2011. Apical ectodermal ridge morphogenesis in limb development is controlled by Arid3b-mediated regulation of cell movements. *Development* **138**:1195-1205.
- 725
- 726
- 727 46. **Takebe A, Era T, Okada M, Martin Jakt L, Kuroda Y, Nishikawa S.** 2006. Microarray analysis of PDGFR alpha+ populations in ES cell differentiation culture identifies genes involved in differentiation of mesoderm and mesenchyme including ARID3b that is essential for development of embryonic mesenchymal cells. *Dev Biol* **293**:25-37.
- 728
- 729
- 730
- 731 47. **Akhavantabasi S, Sapmaz A, Tuna S, Erson-Bensan AE.** 2012. miR-125b targets ARID3B in breast cancer cells. *Cell Struct Funct* **37**:27-38.
- 732
- 733 48. **Joseph S, Deneke VE, Cowden Dahl KD.** 2012. ARID3B induces tumor necrosis factor alpha mediated apoptosis while a novel ARID3B splice form does not induce cell death. *PLoS One* **7**:e42159.
- 734
- 735
- 736 49. **Kobayashi K, Era T, Takebe A, Jakt LM, Nishikawa S.** 2006. ARID3B induces malignant transformation of mouse embryonic fibroblasts and is strongly associated with malignant neuroblastoma. *Cancer Res* **66**:8331-8336.
- 737
- 738
- 739 50. **Kobayashi K, Jakt LM, Nishikawa SI.** 2013. Epigenetic regulation of the neuroblastoma genes, Arid3b and Mycn. *Oncogene* **32**:2640-2648.
- 740
- 741 51. **Oguz Erdogan AS, Ozdemirler N, Oyken M, Alper M, Erson-Bensan AE.** 2014. ARID3B expression in primary breast cancers and breast cancer-derived cell lines. *Cell Oncol (Dordr)* **37**:289-296.
- 742
- 743 52. **Samyesudhas SJ, Roy L, Cowden Dahl KD.** 2014. Differential expression of ARID3B in normal adult tissue and carcinomas. *Gene* **543**:174-180.
- 744

- 745 53. **Nakamura H, Lu M, Gwack Y, Souvlis J, Zeichner SL, Jung JU.** 2003. Global changes in Kaposi's  
746 sarcoma-associated virus gene expression patterns following expression of a tetracycline-  
747 inducible Rta transactivator. *J Virol* **77**:4205-4220.
- 748 54. **Brulois KF, Chang H, Lee AS, Ensser A, Wong LY, Toth Z, Lee SH, Lee HR, Myoung J, Ganem D, Oh**  
749 **TK, Kim JF, Gao SJ, Jung JU.** 2012. Construction and manipulation of a new Kaposi's sarcoma-  
750 associated herpesvirus bacterial artificial chromosome clone. *J Virol* **86**:9708-9720.
- 751 55. **Sturzl M, Gaus D, Dirks WG, Ganem D, Jochmann R.** 2013. Kaposi's sarcoma-derived cell line SLK  
752 is not of endothelial origin, but is a contaminant from a known renal carcinoma cell line. *Int J*  
753 *Cancer* **132**:1954-1958.
- 754 56. **Myoung J, Ganem D.** 2011. Generation of a doxycycline-inducible KSHV producer cell line of  
755 endothelial origin: Maintenance of tight latency with efficient reactivation upon induction.  
756 *Journal of Virological Methods* **174**:12-21.
- 757 57. **Baquero-Perez B, Whitehouse A.** 2015. Hsp70 Isoforms Are Essential for the Formation of  
758 Kaposi's Sarcoma-Associated Herpesvirus Replication and Transcription Compartments. *PLoS*  
759 *Pathog* **11**:e1005274.
- 760 58. **Vieira J, O'Hearn PM.** 2004. Use of the red fluorescent protein as a marker of Kaposi's sarcoma-  
761 associated herpesvirus lytic gene expression. *Virology* **325**:225-240.
- 762 59. **Huang da W, Sherman BT, Lempicki RA.** 2009. Systematic and integrative analysis of large gene  
763 lists using DAVID bioinformatics resources. *Nat Protoc* **4**:44-57.
- 764 60. **Huang da W, Sherman BT, Zheng X, Yang J, Imamichi T, Stephens R, Lempicki RA.** 2009. Extracting  
765 biological meaning from large gene lists with DAVID. *Curr Protoc Bioinformatics* **Chapter 13**:Unit  
766 13 11.
- 767 61. **Gould F, Harrison SM, Hewitt EW, Whitehouse A.** 2009. Kaposi's sarcoma-associated herpesvirus  
768 RTA promotes degradation of the Hey1 repressor protein through the ubiquitin proteasome  
769 pathway. *J Virol* **83**:6727-6738.
- 770 62. **Hughes DJ, Wood JJ, Jackson BR, Baquero-Perez B, Whitehouse A.** 2015. NEDDylation Is Essential  
771 for Kaposi's Sarcoma-Associated Herpesvirus Latency and Lytic Reactivation and Represents a  
772 Novel Anti-KSHV Target. *PLoS Pathog* **11**:e1004771.
- 773 63. **Nelson JD, Denisenko O, Bomsztyk K.** 2006. Protocol for the fast chromatin immunoprecipitation  
774 (ChIP) method. *Nat Protoc* **1**:179-185.
- 775 64. **Nelson JD, Denisenko O, Sova P, Bomsztyk K.** 2006. Fast chromatin immunoprecipitation assay.  
776 *Nucleic Acids Res* **34**:e2.
- 777 65. **Kumar P, Wood C.** 2013. Kaposi's sarcoma-associated herpesvirus transactivator Rta induces cell  
778 cycle arrest in G0/G1 phase by stabilizing and promoting nuclear localization of p27kip. *J Virol*  
779 **87**:13226-13238.
- 780 66. **Hori T, Osaka F, Chiba T, Miyamoto C, Okabayashi K, Shimbara N, Kato S, Tanaka K.** 1999.  
781 Covalent modification of all members of human cullin family proteins by NEDD8. *Oncogene*  
782 **18**:6829-6834.
- 783 67. **Bennett EJ, Rush J, Gygi SP, Harper JW.** 2010. Dynamics of cullin-RING ubiquitin ligase network  
784 revealed by systematic quantitative proteomics. *Cell* **143**:951-965.
- 785 68. **Soucy TA, Smith PG, Milhollen MA, Berger AJ, Gavin JM, Adhikari S, Brownell JE, Burke KE,**  
786 **Cardin DP, Critchley S, Cullis CA, Doucette A, Garnsey JJ, Gaulin JL, Gershman RE, Lublinsky AR,**  
787 **McDonald A, Mizutani H, Narayanan U, Olhava EJ, Peluso S, Rezaei M, Sintchak MD, Talreja T,**  
788 **Thomas MP, Traore T, Vyskocil S, Weatherhead GS, Yu J, Zhang J, Dick LR, Claiborne CF, Rolfe M,**  
789 **Bolen JB, Langston SP.** 2009. An inhibitor of NEDD8-activating enzyme as a new approach to treat  
790 cancer. *Nature* **458**:732-736.

- 791 69. **Blank JL, Liu XJ, Cosmopoulos K, Bouck DC, Garcia K, Bernard H, Tayber O, Hather G, Liu R,**  
792 **Narayanan U, Milhollen MA, Lightcap ES.** 2013. Novel DNA damage checkpoints mediating cell  
793 death induced by the NEDD8-activating enzyme inhibitor MLN4924. *Cancer Res* **73**:225-234.  
794 70. **Ma T, Chen Y, Zhang F, Yang CY, Wang S, Yu X.** 2013. RNF111-dependent neddylation activates  
795 DNA damage-induced ubiquitination. *Mol Cell* **49**:897-907.  
796 71. **Hannah J, Zhou P.** 2009. Regulation of DNA damage response pathways by the cullin-RING  
797 ubiquitin ligases. *DNA Repair (Amst)* **8**:536-543.  
798 72. **Le-Trilling VT, Megger DA, Katschinski B, Landsberg CD, Ruckborn MU, Tao S, Krawczyk A, Bayer**  
799 **W, Drexler I, Tenbusch M, Sitek B, Trilling M.** 2016. Broad and potent antiviral activity of the NAE  
800 inhibitor MLN4924. *Sci Rep* **6**:19977.  
801 73. **Grossmann C, Ganem D.** 2008. Effects of NFkappaB activation on KSHV latency and lytic  
802 reactivation are complex and context-dependent. *Virology* **375**:94-102.  
803 74. **Lei X, Bai Z, Ye F, Xie J, Kim CG, Huang Y, Gao SJ.** 2010. Regulation of NF-kappaB inhibitor  
804 IkkappaBalpha and viral replication by a KSHV microRNA. *Nat Cell Biol* **12**:193-199.  
805 75. **Jin Y, He Z, Liang D, Zhang Q, Zhang H, Deng Q, Robertson ES, Lan K.** 2012. Carboxyl-terminal  
806 amino acids 1052 to 1082 of the latency-associated nuclear antigen (LANA) interact with RBP-  
807 Jkappa and are responsible for LANA-mediated RTA repression. *J Virol* **86**:4956-4969.  
808 76. **Kaul R, Verma SC, Robertson ES.** 2007. Protein complexes associated with the Kaposi's sarcoma-  
809 associated herpesvirus-encoded LANA. *Virology* **364**:317-329.  
810 77. **Li Q, He M, Zhou F, Ye F, Gao SJ.** 2014. Activation of Kaposi's sarcoma-associated herpesvirus  
811 (KSHV) by inhibitors of class III histone deacetylases: identification of sirtuin 1 as a regulator of  
812 the KSHV life cycle. *J Virol* **88**:6355-6367.  
813 78. **Schmid M, Speiseder T, Dobner T, Gonzalez RA.** 2014. DNA virus replication compartments. *J*  
814 *Virol* **88**:1404-1420.  
815 79. **Krishnan HH, Naranatt PP, Smith MS, Zeng L, Bloomer C, Chandran B.** 2004. Concurrent  
816 expression of latent and a limited number of lytic genes with immune modulation and  
817 antiapoptotic function by Kaposi's sarcoma-associated herpesvirus early during infection of  
818 primary endothelial and fibroblast cells and subsequent decline of lytic gene expression. *J Virol*  
819 **78**:3601-3620.  
820 80. **AuCoin DP, Colletti KS, Cei SA, Papouskova I, Tarrant M, Pari GS.** 2004. Amplification of the  
821 Kaposi's sarcoma-associated herpesvirus/human herpesvirus 8 lytic origin of DNA replication is  
822 dependent upon a cis-acting AT-rich region and an ORF50 response element and the trans-acting  
823 factors ORF50 (K-Rta) and K8 (K-bZIP). *Virology* **318**:542-555.

824

825 **Figure legends**

826 **FIG 1.** Analysis via SILAC coupled to LC-MS/MS of nuclear proteome changes in response to KSHV-  
827 RTA expression. Flp-In-293 cells were used to develop a cell line with doxycycline-inducible FLAG-  
828 tagged RTA expression (iRTA-293). (A) Cells were labeled with R10K8 (heavy) or R0K0 (light)  
829 labelled SILAC media for two weeks. FLAG-RTA expression was induced in heavy-labelled cells for  
830 12 h and these were fractionated into nuclear and cytoplasmic compartments. Fractionation  
831 success was validated by immunoblot analysis using the nuclear (Lamin-B1) and cytoplasmic  
832 (GAPDH) markers. As expected, RTA expression was largely restricted to the nuclear  
833 compartment, and was only found in dox.-treated cells. (B) FLAG-RTA expression was analyzed  
834 by confocal immunofluorescence that revealed all Dox.-treated cells were positive for FLAG-RTA  
835 and Untreated (-Dox; R0K0-labeled cells) were negative for RTA expression, demonstrating tight  
836 regulation of FLAG-RTA. Scale bar - 10  $\mu$ m. (C) KEGG pathway analysis of nuclear proteins that  
837 were upregulated 2-fold or more due to RTA expression, with at least 2 independent peptides  
838 revealed various cellular pathways associated RTA expression. GO Term – gene ontology term.

839

840 **FIG 2.** RTA enhances ARID3B expression. (A) Doxycycline- (Dox.)-induced expression in iRTA-293  
841 cells for 12 h and reactivation of the KSHV lytic cycle by the addition of Dox. in TReX-BCBL1-RTA  
842 cells increased *ARID3B* expression as measured by qRT-PCR. Error bars represent standard  
843 deviation from the mean from three independent biological replicates and quantification was  
844 normalized to *GAPDH* using the  $\Delta\Delta$ Ct method. Student's t-tests were used to determine statistical  
845 significance. Three independent experiments were performed for each cell line (B) Reactivation

846 of the lytic cycle from latently infected iSLK-BAC16 and TReX-BCBL1-RTA cells led to an increase  
847 in ARID3B protein expression. In this experiment, separate immunoblots were used for the  
848 detection of RTA (denoted by a line). (C) Quantification of protein expression in (B) (see Materials  
849 and Methods). Data are derived from two independent experiments and error bars represent  
850 standard deviation of the mean (calculated from technical replicates within independent  
851 experiments). \* =  $P < 0.05$  (Student's t-test).

852 **FIG 3.** ARID3B relocates to KSHV replication compartments upon reactivation of the lytic cycle.  
853 (A) Confocal immunofluorescence analysis demonstrated that ARID3B relocated to discrete,  
854 RTA-positive foci that resemble replication compartments (white arrows) upon Dox.-induced  
855 reactivation of the KSHV lytic cycle in TReX-BCBL1-RTA cells. (B) Further evidence suggesting that  
856 ARID3B relocated to replication compartments demonstrated by its colocalization with RTA and  
857 EdU-positive foci (white arrows). EdU is used as a marker of newly replicated viral (57). Scale bar  
858 - 10  $\mu\text{m}$ .

859 **FIG 4.** ARID3B inhibits KSHV lytic reactivation. (A) Latently infected iSLK-BAC16 cells were  
860 independently transfected with two separate siRNAs pools targeting *ARID3B* (or a non-targeting  
861 scramble control siRNA) for 72 h and then reactivated by addition of dox (a further 24 h; see  
862 Materials and Methods). RT-qPCR was used to quantify *ARID3B*, *ORF57* and *gB* levels and the fold  
863 difference in expression was compared to scramble control using *GAPDH* levels to normalize  
864 between samples. Error bars represent standard deviation from the mean from two independent  
865 experiments, with mean values calculated from the technical replicates of each experiment.  
866 Statistical analyses demonstrated a significant increase in lytic gene expression in siARID3B-  
867 treated cells compared to scramble control \*\*  $p = <0.0001$  (Student's t-test). (B) Knockdown of

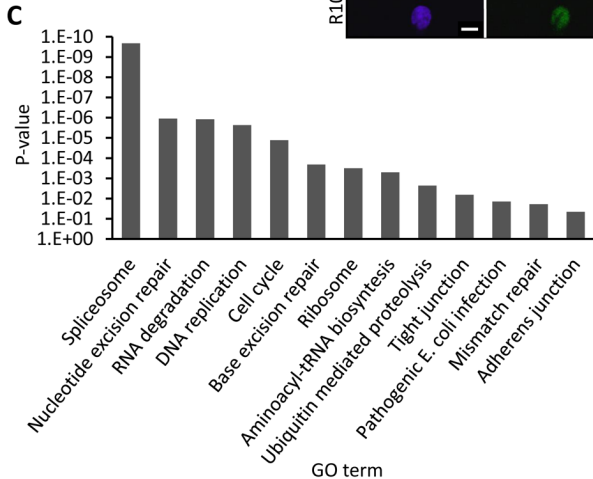
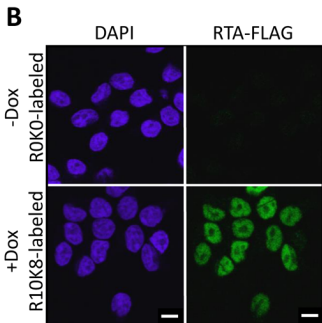
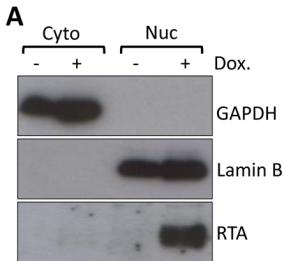
868 ARID3B led to an enhancement of lytic protein expression. (C) Quantification of (B) (see Materials  
869 and Methods). (D) Knockdown of ARID3B enhanced viral genome replication. ARID3B siRNA or  
870 scramble control siRNAs transfection of iSLK-BAC16 cells followed by reactivation of the lytic  
871 cycle for 72 h led to an increase in viral genome replication, as quantified by qPCR of the KSHV  
872 ORF57 gene. Cellular GAPDH was used to normalize between samples and error bars represent  
873 standard deviation from the mean from three independent biological replicates (\*  $p < 0.05$ ). (E)  
874 Knockdown of ARID3B enhances virion production. Media from iSLK-BAC16 cells that had been  
875 transfected with siARID3B or scramble control siRNAs were used to infect KSHV-negative  
876 HEK293T cells. As a measure of infection, RT-qPCR analysis of the KSHV lytic gene *ORF57* was  
877 performed 24 h following infection. Data represent three independent infections in a single  
878 experiment, and Student's t-test was used to determine statistical significance (\* =  $P < 0.05$ ). (F)  
879 Overexpression of FLAG-ARID3B inhibits reactivation of lytic cycle-associated protein expression.  
880 Expression vector containing FLAG-tagged ARID3B (FLAG-ARID3B) or FLAG-SRAG (used as a  
881 negative control) were transfected in to iSLK-BAC16 cells for 24 h, followed by Dox.-induced  
882 reactivation of the KSHV lytic cycle. Cell lysates were harvested 24 h later and subjected to  
883 immunoblot analysis of lytic proteins ORF57 and mCP (minor capsid protein).

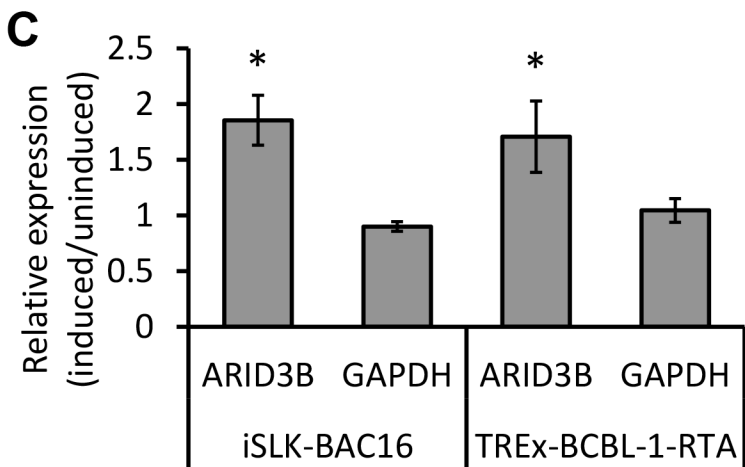
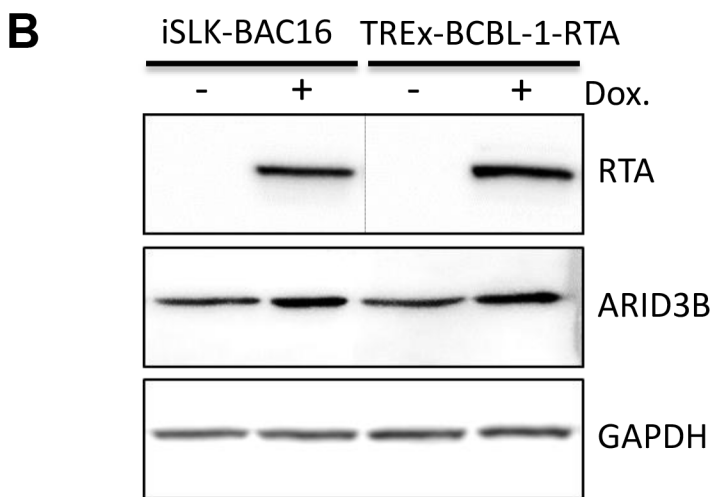
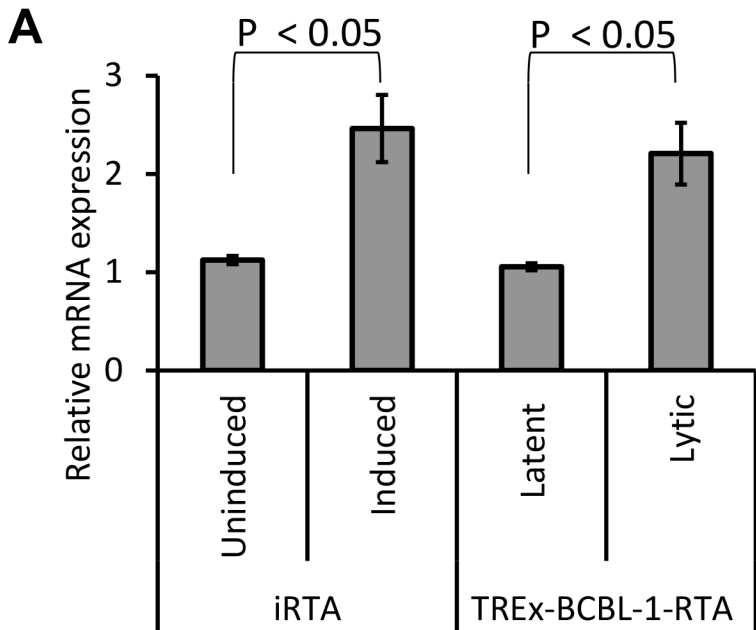
884 **FIG 5.** RTA and ARID3B do not directly interact. Immunoprecipitation assay showing RTA interacts  
885 with known binding partner ORF59, but not ARID3B. The lytic cycle was induced in ARID3B-  
886 transfected iSLK-BAC16 cells. Proteins were immunoprecipitated with the indicated antibodies  
887 followed by immunoblot analysis.

888 **FIG 6.** ARID3B interacts with the KSHV genome in a lytic reactivation-dependent manner. (A) DNA  
889 affinity assays performed according to (25); biotinylated PCR products spanning oriLyt left of

890 KSHV (GenBank accession number: NC\_009333.1) and control DNA amplified from the RTA  
891 coding region were bound to streptavidin Dynabeads and incubated with lysates from  
892 reactivated 293T rKSHV.219 cells expressing FLAG-ARID3B. This suggested ARID3B bound these  
893 sequences with preference for the A/T-rich region. (B) TReX-BCBL1-RTA cells were treated with  
894 doxycycline for 18 h (w/ Dox) to reactivate the lytic cycle or were left untreated (w/o Dox).  
895 Samples were subjected to ChIP with an antibody to ARID3B or normal rabbit IgG and primers  
896 specific for sequences in the A/T-rich region of oriLyt or the RTA coding region. The percentage  
897 of output versus input DNA was calculated and is presented relative to normal rabbit IgG values  
898 from unreactivated (w/o Dox) cells (set to 1). Data represent two biological (i.e. independent  
899 ChIPs) and two technical replicates per ChIP from a single experiment, and values are given as  
900 the mean  $\pm$  standard deviation. Student t-tests were used to determine statistical significance.

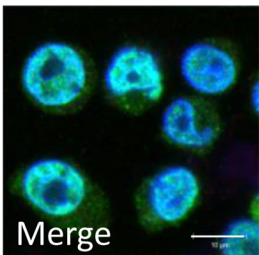
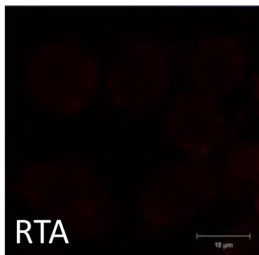
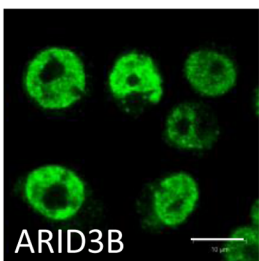
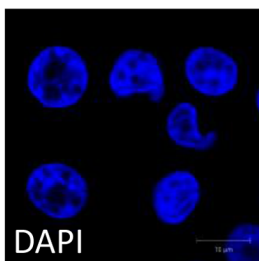
901 **FIG 7.** A model of how ARID3B inhibits lytic reactivation. Periodic reactivation of KSHV involves  
902 replication of the viral genome and the production of new virions, a necessary step for the  
903 maintenance of latency and the pathogenesis of KS (2). Viral DNA replication initiates from the  
904 *cis*-acting oriLyt where proteins essential for this process are recruited. These include viral  
905 proteins RTA, K8 and the six core proteins (DNA polymerase, DNA processivity factor etc.) (80) in  
906 addition to various cellular *trans*-acting proteins (25). We hypothesize that during reactivation  
907 RTA is expressed leading to the enhanced expression of ARID3B and its recruitment to viral  
908 genomes, specifically AT-rich elements such as those found in oriLyt. ARID3B may compete with  
909 factors required for reactivation for binding with the KSHV genome in order to modulate the  
910 levels of reactivation or for the establishment of latency.



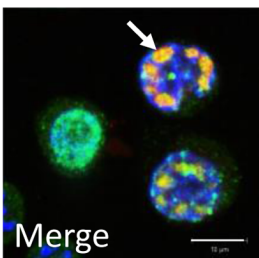
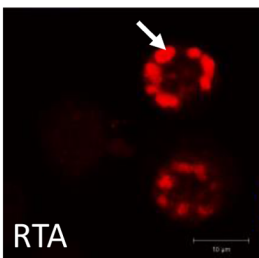
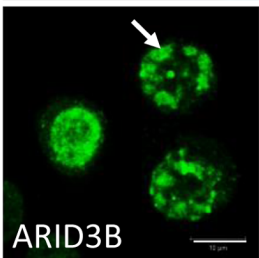
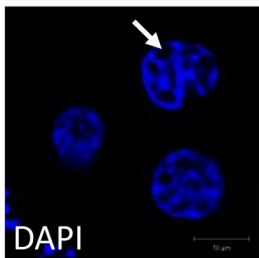
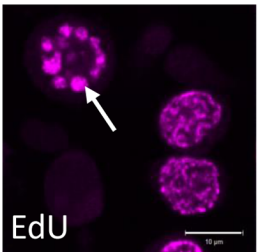
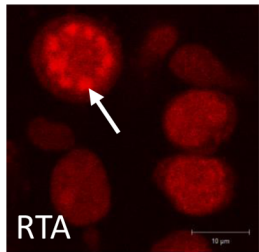
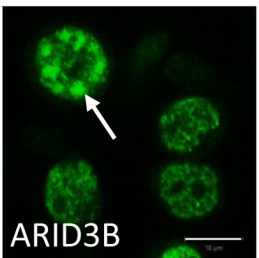
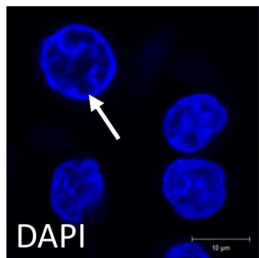


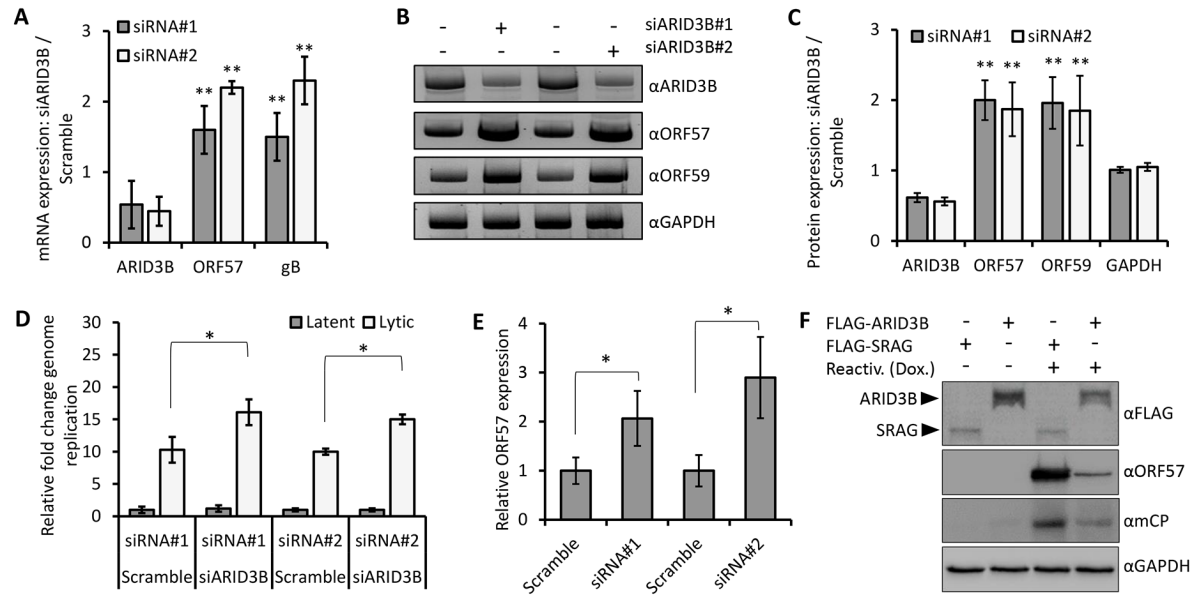
**A**

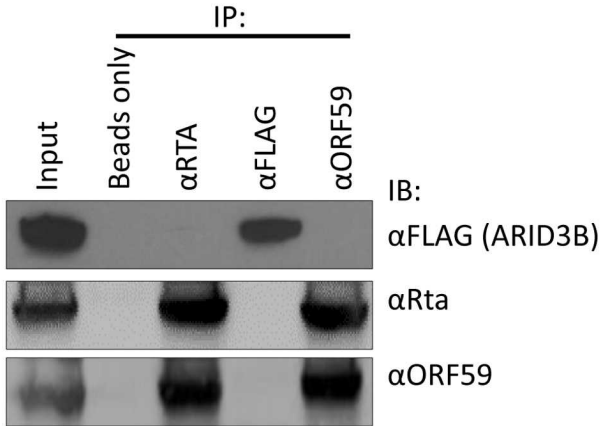
-Dox (latent)



+Dox (lytic)

**B**





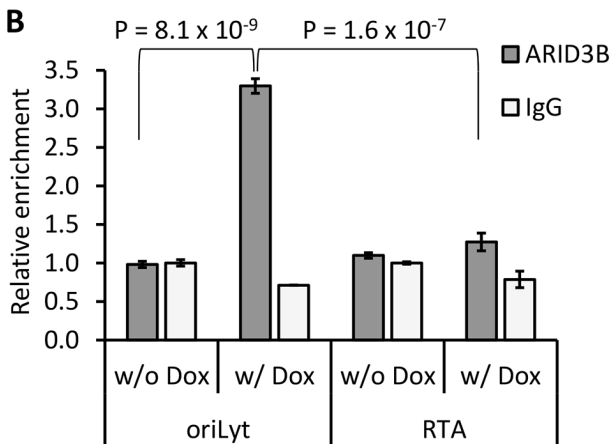
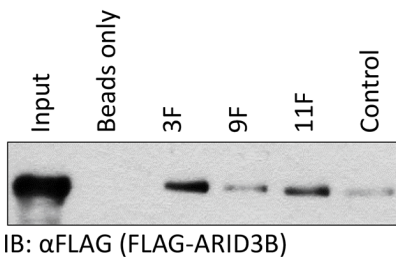
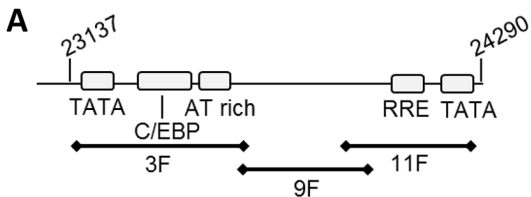


**TABLE 1** Top 15 proteins increased in abundance in the nuclear fraction upon RTA expression.

Name	Uniprot ID*	Fold increase	Unique peptides	Sequence coverage (%)	PEP**	Function*
ATPase family AAA domain-containing protein 3B	Q5T9A4-1	53.4	12	19.8	1.90E-79	May play a role in a mitochondrial network organization typical for stem cells.
Cell division cycle-associated 7-like protein	Q96GN5-1	15.5	3	9.3	1.68E-18	Transcriptional repressor.
Transmembrane protein 43	Q9BTV4	11.9	7	24.8	1.18E-55	May have a role in maintaining nuclear envelope structure.
Kinesin-like protein KIF11	P52732	11.7	37	46.14	6.53E-283	Motor protein required for establishing a bipolar spindle during mitosis.
BAT2 domain-containing protein 1	Q9Y520-7	10.8	39	17	1.39E-164	Unknown.
Centrosomal protein of 170 kDa	Q5SW79-1	9.6	19	14.3	2.53E-66	Plays a role in microtubule organization.
Uncharacterized protein KIAA1671	Q9BY89-1	9.3	4	2.6	3.61E-11	Unknown.
Upstream of NRAS	Q68DF1	9.1	18	26.1	2.26E-193	May be involved in translationally coupled mRNA turnover.
AT-rich interactive domain-containing protein 3B	Q8IVW6-1	7.5	8	15.7	2.25E-67	Transcription factor which may be involved in neuroblastoma growth and malignant transformation.
General transcription factor 3C polypeptide 2	Q8WUA4-1	7.5	3	5.5	1.88E-10	Required for RNA polymerase III-mediated transcription.

Protein LYRIC	Q86UE4	7.0	4	7.7	2.99E-14	Activates the NF-κB transcription factor.
Cadherin-2	P19022	6.4	3	5.8	2.33E-11	Calcium-dependent cell adhesion proteins.
Cytospin-A	Q69YQ0	6.1	3	3.3	3.88E-10	Involved in cytokinesis and spindle organization.
Lethal(3)malignant brain tumor-like 3 protein	Q96JM7-1	5.7	3	4	3.46E-07	Putative Polycomb group (PcG) protein. PcG proteins maintain the transcriptionally repressive state of genes.
Lysine-specific demethylase 2A	Q9Y2K7-1	5.2	3	2.8	8.35E-08	Histone demethylase that specifically demethylates 'Lys-36' of histone H3. Maintains heterochromatin.

---

\* Protein information was annotated from the Uniprot database ([www.uniprot.org](http://www.uniprot.org)).

\*\* Posterior error probability (a statistical measure for peptide identification – should be below 0.1).

**TABLE 2** Ingenuity Pathway Analysis (IPA) of the top canonical pathways associated with RTA expression (nuclear proteome).

Name	P-value
Transcriptional Repression	2.85E <sup>-8</sup>
Aminoacyl-tRNA Biosynthesis	3.87E <sup>-5</sup>
Cell Cycle Control of Chromosomal Replication	7.64E <sup>-4</sup>
Mismatch Repair in Eukaryotes	7.84E <sup>-4</sup>
Role of BRCA1 in DNA Damage Response	8.12E <sup>-4</sup>